Flood Modelling in Pasig-Marikina River Basin

Roy A. Badilla
March, 2008

Flood Modelling in Pasig-Marikina River Basin

by

Roy A. Badilla

Thesis submitted to the International Institute for Geo-information Science and Earth Observation in partial fulfilment of the requirements for the degree of Master of Science in Geo-information Science and Earth Observation, Specialisation: Integrated Watershed Modelling and Management

Thesis Assessment Board

Chairman	Prof. Dr. Ir. Z. Su
External Examiner	Dr. M. Krol (University of Twenty)
First Supervisor	Dr. Ing. T.H.M. Rientjes
Second Supervisor	Alemseged Tamiru Haile, M.Sc.

INTERNATIONAL INSTITUTE FOR GEO-INFORMATION SCIENCE AND EARTH OBSERVATION
ENSCHEDE, THE NETHERLANDS

Disclaimer

Dedicated to my wife Denise
and children Carlo and Daniel

and

to my loving mother Pacing
and my departed father Itchoy

Abstract

The Metropolitan Manila has been experiencing recurrent flooding especially in the low lying areas along the Pasig-Marikina River. Because of this problem, the Philippine government has implemented several projects to achieve effective flood control operations in the area. The first project to be completed was the construction of Mangahan floodway. However, after the completion of the project, informal settlers have started building their houses in the side slope of the floodway making it risky to operate the Rosario Weir. Rosario Weir is the structure that controls the inflow to the Mangahan Floodway. This study focuses on the development of a HBV model and a DUFLOW model to study the flood wave behaviour in the study area and to come up with calibrated models which could be used as basis for the operation of Rosario Weir and Napindan Hydraulic Control Structure for effective flood control and early warning in Mangahan Floodway. The HBV-96 model was applied to simulate the runoff from Pasig-Marikina River Basin using hourly hydrometeorological data. Four rainfall stations and one water level station for a period of three years were used for the calibration and validation of the model. The catchment was extracted from SRTM elevation data and was divided into six subbasins. Land cover classes applied for this study were field and forest. Other land cover classes that can be specified in the HBV model do not apply to the study area. Two modules of the DUFLOW model were used for this study; the water quantity module and the RAM module. The DUFLOW water quantity module was setup using twelve river cross sections along the upper Marikina River with a river length of 20.10 kilometers. However, the distances between river cross sections along the river length is not uniform. Water level data from Montalban water level station was used as the upstream boundary condition and the data from Mangahan water level station was used as the downstream boundary condition. The calibration of the DUFLOW water quantity module was done at Marikina water level station. Inflow from the intermediate area between the upstream boundary node and the calibration node was handled by RAM module. However, no calibration was done in RAM module because of unavailability of in-situ data although model parameters were specified based on a priori knowledge about the site characteristics. After the DUFLOW calibration, the hydrograph from the HBV model simulation was used as the upstream boundary condition while the downstream boundary condition remains the same. The purpose of integrating the result of the HBV model to the DUFLOW model is to increase the flood lead time which could be beneficial for flood control and early warning purposes. The results obtained from this research were satisfactory giving a Nash-Sutcliffe efficiency coefficient (R^2) of 0.79 and 0.76 for the HBV model calibration and validation data set, respectively. The DUFLOW model was more accurate with R^2 of 0.91 for the model that used the Montalban observed water level data and 0.90 for the model that used the simulated HBV hydrograph. Hence, the calibrated models can be applied for the flood control and early warning system in Mangahan Floodway.

Keywords: Pasig-Marikina River Basin, Upper Marikina River, Rosario Weir, Napindan Hydraulic Control Structure, Mangahan Floodway

Acknowledgements

I would like to thank the Government of the Netherlands through the Netherlands Fellowship Programme (NFP) for granting me this opportunity to study for a Master of Science degree. I am also grateful to my employer, the Philippine Atmospheric, Geophysical and Astronomical Services Administration (PAGASA) for giving me this opportunity to pursue a higher education.

My sincere thanks to my first supervisor, Dr. Ing. Tom Rientjes, for his patience, guidance and critical comments on my work. I also thank him for spending unlimited time during meetings and consultations. I am also grateful to my second supervisor, Alemseged Tamiru Haile, MSc, for unselfishly sharing his knowledge and encouragements. Rest assured that the knowledge that I have gained from this study will be fully applied in my home country. Thank you very much to both of you.

Furthermore, I would like to thank the WREM staff for their unwavering support for the whole duration of my study. To my fellow WREM students, thank you for the new found friendship and for the comfort during the times when life becomes rough. It makes me strong because I know that you are always there ready to lend your helping hands.

I am greatly indebted to Engr. Emma Quiambao (EFCOS/MMDA) and her kind staff for providing me the much needed data for this study. I would also acknowledge the help of Ms. Alma Arquero (GIS Division/ NAMRIA) who provided the digital copy of the land cover map and Engr. Jessie Felizardo for some useful information regarding the study area. This study was made possible because of the data and information you have provided.

I am also grateful to the employees of the Flood Forecasting Branch (FFB/PAGASA) for their support during the fieldwork campaign especially Dr. Susan Espinueva, Marivic Marica, Jun Paat, Sheila Sy, Pabling Villablanca and Vicky Mendoza.

Moreover, I would like to thank my family for their prayers, support and understanding. I would also acknowledge the help and support of my Filipino family here in Enschede.

Finally, above all things, I want to thank GOD for everything that I have.

Table of contents

Abstract i
Acknowledgements ii
List of Figures v
List of Tables vi
1. Introduction 1
1.1. Flood 1
1.2. Thesis Structure 4
2. Study Area 5
2.1. Background 5
2.2. Description of Study Area 6
2.3. Mangahan Floodway Early Warning System 8
2.4. Weather and Climate 10
2.5. Topography 10
2.6. Problem Statement 11
2.7. Research Objectives 12
2.7.1. General 12
2.7.2. Specifics 12
2.7.3. Research Questions 12
3. Literature Survey 13
3.1. Hydrologic Cycle at Catchment Scale 13
3.2. Runoff Processes 14
3.3. Hydrologic and Hydraulic Modelling 15
3.4. Flood Modelling 16
3.5. Remote Sensing and Geographic Information System in Flood Modelling 17
3.6. Previous Study in the Area 18
4. Materials and Methodology 19
4.1. General Methodology 19
4.2. HBV Model 20
4.2.1. Model Background 20
4.2.2. Model Structure 20
4.2.3. Model Routines 22
4.2.4. Model Calibration 24
4.2.5. Model Setup 25
4.3. DUFLOW Model 28
4.3.1. Model Background 28
4.3.2. Initial and Boundary Conditions 30
4.3.3. Model Calibration 30
4.3.4. Model Setup 30
4.4. Data Availability and Preparation 33
4.4.1. SRTM Elevation Data 33

4.4.2. Catchment Extraction from DEM 35
4.4.3. Rainfall Data 35
4.4.4. Water Level Data 36
4.4.5. Land Cover Data 37
4.4.6. River Cross Sections 37
5. Results and Discussions 39
5.1. HBV Model 39
5.1.1. Model Performance 39
5.1.2. Model Uncertainty 41
5.1.3. Sensitivity Analysis 42
5.2. DUFLOW Model 44
5.2.1. RAM Precipitation Runoff Module 44
5.2.2. DUFLOW Water Quantity Module 45
5.2.3. Model Uncertainty 48
5.2.4. Sensitivity Analysis 48
5.2.5. Model Stability 49
6. Conclusions and Recommendations 51
6.1. Conclusions 51
6.2. Recommendations 52
References 53
Appendix 57
Appendix A: List of Acronyms 58
Appendix B: Classification of Flood Phase 59
Appendix C: Principles of Flood Operation 60
Appendix D: Flood Warning Announcements 61

List of Figures

Figure 1: Location of the study area 5
Figure 2: Pasig-Marikina River Basin and its river systems 6
Figure 3: The Rosario Weir 7
Figure 4: EFCOS telemetry and warning systems 9
Figure 5: Climate of the Philippines 10
Figure 6: Part of Mangahan Floodway showing informal settlers on the side slopes of the floodway .11
Figure 7: Major processes of the schematized hydrologic cycle at a catchment scale 13
Figure 8: Schematization of runoff processes in a sloping area at a catchment scale 14
Figure 9: General methodology flowchart 19
Figure 10: Schematic diagram of HBV-96 model structure 21
Figure 11: Schematization of soil moisture parameters 22
Figure 12: Schematization of the outflow from upper and lower reservoirs 23
Figure 13: Schematization of transformation function parameters 24
Figure 14: Schematization of model input/output in the HBV model 25
Figure 15: Pasig-Marikina River Basin divided into different subbasins 26
Figure 16: Schematization of model input/output in the DUFLOW water quantity module 32
Figure 17: DUFLOW model network 32
Figure 18: Rainfall homogeneity test 36
Figure 19: Reclassified land cover map 37
Figure 20: Survey group conducting river cross sectioning activities 38
Figure 21: HBV model calibration result shown as discharge hydrograph 40
Figure 22: HBV model calibration result shown as water level hydrograph 40
Figure 23: HBV model validation result shown as discharge hydrograph 41
Figure 24: HBV model validation result shown as water level hydrograph 41
Figure 25: Relation between *Alfa* and Nash-Sutcliffe efficiency coefficients (R^2) 43
Figure 26: Relation between *FC* and Nash-Sutcliffe efficiency coefficients (R^2) 43
Figure 27: Relation between *Khq* and Nash-Sutcliffe efficiency coefficients (R^2) 44
Figure 28: Simulated hydrograph using the minimum value of *Khq* 44
Figure 29: Lateral inflows from intermediate areas computed from RAM module 45
Figure 30: DUFLOW model calibration result using Montalban water level data 46
Figure 31: DUFLOW model result using the simulated hydrograph of HBV 47
Figure 32: Comparison of the DUFLOW model results 47
Figure 33: Relation between *k* values and simulated peaks 49
Figure 34: Comparison of hydrographs using high and low *k* values 49

List of Tables

Table 1: Natural disasters and accidents in WHO European Region, 1990 to 2006 2
Table 2: Some spectral bands used in remote sensing and its principal applications 18
Table 3: Subbasin areas used in the HBV model 26
Table 4: Land cover zones and areas in each subbasin 27
Table 5: Weights of rainfall stations in each subbasin 27
Table 6: List of parameters used in the HBV calibration 28
Table 7: Weights of rainfall stations in each area used in RAM module 31
Table 8: Parameters used in unpaved surface in RAM module 31
Table 9: SRTM data naming conventions 34
Table 10: Performance requirements for the SRTM data products 34
Table 11: Summary of SRTM data performance 34
Table 12: Rainfall stations, location coordinates and elevations 36
Table 13: Best parameter set used in HBV model 39
Table 14: Parameter values used in unpaved surface in RAM Module 45

1. Introduction

1.1. Flood

The United States Geological Survey (2007) defines a flood *as relatively high water that overflows the natural or artificial banks of a stream or coastal area that submerges land not normally below water*. Flood is a natural phenomenon that occurs when the volume of water flowing in a system exceeds its total water holding capacity. The word flood originates from an old English word *flod*, a word comparable to German's *flut* and Dutch's *vloed* (Wikipedia, 2007b).

United Nations defined flood *as an excess flowing or overflowing of water, especially over land which is not normally submerged* (ESCAP/UN, 1997). This natural phenomenon can have several sources such as; prolonged rain with considerable intensity, dam or dike break, river blockages, storm surges, abnormally high tides and tidal waves or tsunamis.

ESCAP/UN (1997) outlined the important characteristics of floods which determine the magnitude and cost of their disastrous effect. The list includes the following:

- The peak depth of inundation, which determines the extent and cost of damage to buildings and crops and the cost and feasibility of mitigation measures;
- The aerial extent of inundation, which determines similar factors;
- The duration of flooding, which is an important factor in determining the degree of damage and inconvenience caused;
- The rate of rise of the flood event, which determines the effectiveness of flood warning and evacuation procedures;
- The velocity of flood flow, which determines the cost of flood damage and the feasibility and design of levees and flood proofing structures;
- The frequency of flooding, which expresses the statistical characteristics of flood events of a given magnitude and determines the long-term average costs and benefit of flooding and flooding mitigation; and
- The seasonability of flooding, which determines the cost of flood damages particularly when agricultural areas are inundated.

In recent history, floods are becoming more frequent and severe and some organizations even counted it as the most damaging natural disaster in a region. In Europe, flooding is the most common natural disaster and the most costly in economic terms as shown in Table 1. The Emergency Disasters Data Base (EM-DAT) has recorded a total of 238 flood events in European region from 1975 to 2001. In the last decade, 1,940 people died due to flooding and 417,000 were left homeless. Europe experienced eight major floods on January to July 2002 which made 93 people perished and 336,000 persons affected with damages estimated to reach US$ 480 million (WHO/Europe, 2002).

Table 1: Natural disasters and accidents in WHO European Region, 1990 to 2006

Type of Event	Number of Events	Deaths	Affected Population	Economic Damages (Thousands of USD)
Drought	31	2	14,865,575	14,297,309
Earthquake	102	21,840	5,875,138	30,225,449
Extreme Temperature	112	52,119	1,389,529	9,024,788
Flood	344	3,593	11,566,509	66,093,052
Accident	609	16,856	137,638	11,697,048
Landslide/Avalanche	57	2,084	90,196	156,586
Wild Fire	58	228	286,969	3,540,357
Wind Storm	170	1,397	8,063,234	33,114,822
Total	1,483	98,119	42,274,788	168,149,414

Source: WHO/Europe (2007)

Also the United States of America were not spared from the damaging effect of floods. In the 20th century, floods were recorded as the number one disaster in terms of human lives lost and damages to property (Perry, 2000). Hurricane Katrina, which affected part of the United States of America during late summer of 2005, set the record as the costliest natural disaster in the US history. The damages caused by hurricane Katrina which also caused a remarkable flooding reached a record of US$ 200 billion (USGS, 2006). Floods claim about 140 lives and US$ 6 billion in property damages each year.

In Africa, it was estimated that about 2.5 million people have been affected in over 14 countries across the African continent during the September 2007 flood. It was reported that 250 people perished during this flood event which was considered as one of the worst flooding in recorded history (Wikipedia, 2007a).

Asia is one of the most disaster prone regions in the world experiencing almost all types of natural hazards. Floods topped the list of natural disasters in terms of damages to properties and losses of human lives. The June 2007 flood that hit China has affected around 200 million people and is said to be the worst flooding in more than 50 years (ReliefWeb, 2007). The July and August 2007 flood that hit South Asia was one of the worst monsoons flooding in living memory (UNICEF, 2007). This flood affected countries of India, Bangladesh and Nepal. The said flood claimed more than 300 lives and affected some 20 million people.

Some parts of the Philippines including Metropolitan Manila are flood prone areas because of its geographical location and low elevations. Recurrent flooding is experienced in those places especially during rainy season or whenever rain bearing weather disturbance affects the country. A massive flooding was experienced on August 2004 in areas of Metropolitan Manila and nearby provinces when two typhoons simultaneously affected the country. In metropolitan Manila, the floods affected a total of 24,108 persons with 8 people perished. In nearby provinces, flood depth of two to twelve feet submerged some 960 villages in 11 cities and 86 towns affecting around 930,500 people (IFRC, 2004).

The frequency of occurrence and the intensity of damages and losses of lives resulting from floods made it known all over the world that flood is a great treat to humanity. However, since serious floods occur in a certain location with a return period of years or decades, the lessons learned from previous flood may have been forgotten (Miller, 1997). Miller (1997) also pointed out that flood has accounted for about one third of the 5,370 natural disasters that occur in the year 1986 to 1995 and claimed 55 percent of the 367,000 people that perished. Windstorms were responsible for another one third but most of them, such as hurricanes and tropical cyclones also induce floods.

The direct effects of floods includes; losses of lives, damage to property, disruption of transportations, communications, health and community services, crop and livestock damages, and interruptions and losses in businesses. The indirect effects of floods are far more damaging. The negative impact to economy in countries frequented by floods is usually severe especially if it is a poor or a developing country.

The traumatic consequence of floods has called for the growing attention because of the need to prevent or control flood damages in our society. Mitigating flood damages can be drawn in two possible ways; structural measures and non-structural measure (ESCAP/UN, 1991). Structural measures include the building of dikes, dams and reservoirs and channel improvements designed to reduce the incidence or extent of flooding. Structural mitigation measures are methods designed to divert flood water away from the people. This type of mitigation measures are proven effective but most often expensive.

The non-structural method of mitigating flood damages place people away from the flood. This method is designed to reduce the impact of flooding to society and economy and includes; flood insurance, land use planning and zoning and flood forecasting and warning schemes. Hydrologic/hydraulic models are often used in flood forecasting and early warning systems. These models when optimally calibrated and validated can be an effective tool in mitigating flood damages through non-structural means.

Flood modelling which started from a very simple lumped model during its infancy days has now become very sophisticated with advances in remote sensing and geographic information system. During the early days of flood modelling, the usual problem that a modeller encountered was the inadequacy of data. Detailed information regarding the hydrometeorological and topographical characteristics of a catchment is usually not known. However, with the introduction of remote sensing and geographic information system, data scarcity problem was addressed. Nowadays, physically based – fully distributed models can be executed. Another advancement in science which help improved flood modelling and forecasting was the development of rainfall estimation algorithms which can be entered into a flood model. These algorithms help extend the lead time in flood forecasting and is most useful for flash flooding rivers.

Flood is one of the most distractive and devastating natural phenomena on earth, but its devastation can be greatly lessen if a judicious mix of both the structural and non-structural measures are introduced.

FFB/PAGASA (2002)

The study area, the Pasig-Marikina River Basin, is located east of Metropolitan Manila. This basin is the source of flood waters that inundates low lying areas along the Pasig-Marikina River and Mangahan Floodway. Presently, there is an existing telemetering system that links remote rainfall and water level stations to the monitoring agency. Warning posts with voice warnings and sirens were installed along the left and right banks of Mangahan Floodway. However, no flood model is currently used for flood early warning operations.

1.2. Thesis Structure

This thesis consists of six chapters and is mainly focused on the development of a flood model that could be used as basis for the operation of flood control structures in Mangahan Floodway (Rosario Weir) and in Napindan Channel (Napindan HCS) for the EFCOS' flood control activities.

Chapter two is focused on the description of the study area, river systems and other water bodies, hydraulic structures, topography, weather and climate, telemetry and warning systems in the area. Also included in this chapter are; Problem statement, research objectives and research questions.

Chapter three is devoted to literature survey. This includes some backgrounds and discussions on hydrologic cycle at catchment scale, runoff processes, flood modelling, hydrologic and hydraulic modelling and the importance of remote sensing and geographic information system in flood modelling. Previous studies on the area also form part of this chapter.

Chapter four describes the materials and methods used in this research. Description of the models used and the model setup adopted is the main part of this chapter. Descriptions and sources of data used can also be found here. Chapter five focuses on the presentation and discussion of results and Chapter six contains the conclusions and recommendations.

2. Study Area

2.1. Background

The Republic of the Philippines is an archipelago located in southeast of the mainland Asia between 4°23'N and 21°25'N latitude and 112°E and 127°E longitude. Consisting of some 7,107 islands, it covers a total land area of 300,000 square kilometers. It is bounded by the South China Sea on its northern and western sides, the Celebes Sea in the south, and the Pacific Ocean in the east. Its total length is about 1,850 kilometers starting from the point near the southern tip of Taiwan and ending close to northern Borneo. Its breadth is about 965 kilometers. The Philippines has a total coastline of 17,500 kilometers.

There are three major island groups that form part of the Philippines: Luzon, Visayas and Mindanao as shown in Figure 1 (left image). The country is divided into 17 administrative regions, 78 provinces, 115 cities, 1,496 municipalities, and 41,939 villages. The topography of the bigger islands, particularly Luzon and Mindanao is characterized by alluvial plains, narrow valleys, rolling hills and high mountains. The highest mountains are found in Luzon and Mindanao, with the altitudes varying from 1,790 to 3,144 meters. The smaller islands are mountainous in the interior, surrounded by narrow strips of discontinuous flat lowlands which constitute the coastal rims. The shorelines of both large and small islands are irregular. More than half of the total population lives in the island of Luzon while the rest is almost equally divided between Visayas and Mindanao.

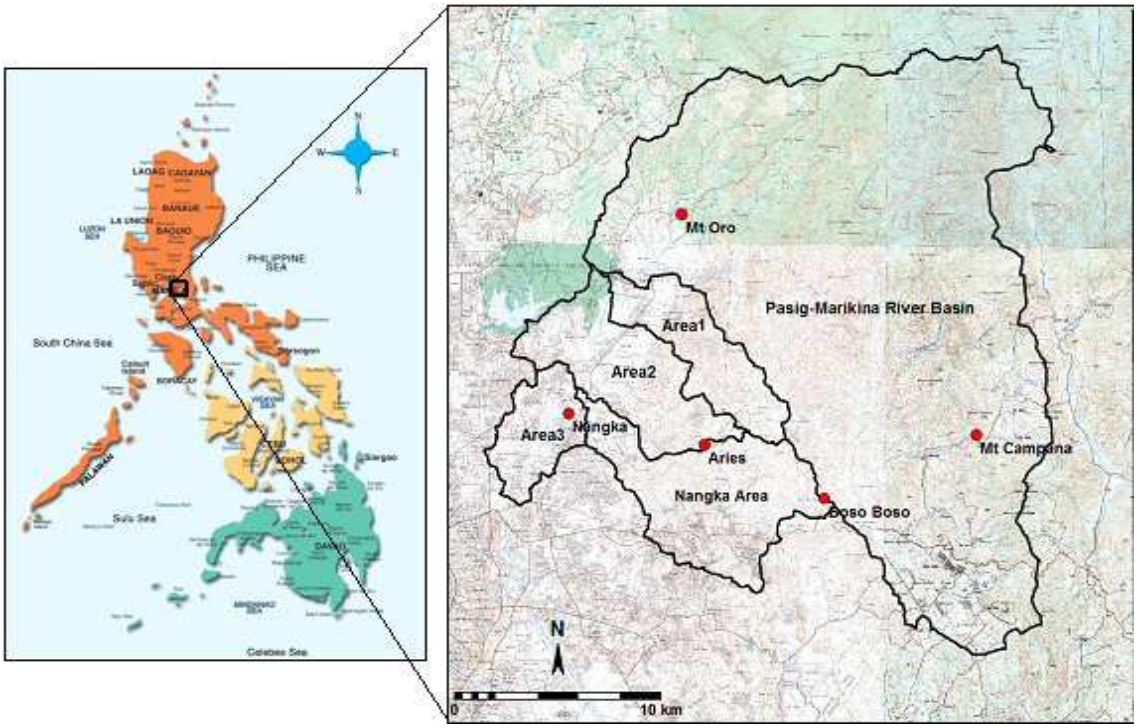

Figure 1: Location of the study area

Nearly 12 million people (about 16 percent of the total population) reside in Metropolitan Manila, the capital region. The total population of the Philippines for the year 2010 is expected to reach 94 million (Ericta, 2006).

2.2. Description of Study Area

Pasig-Marikina River Basin

The Pasig-Marikina River Basin is located east of Metropolitan Manila and has a total drainage area of 377.82 square kilometers. It drains through Marikina River then to Pasig River and out to Manila Bay. It serves as the head water that causes floods in the low lying areas of Metropolitan Manila along the Pasig-Marikina River. Most of the flood water that cascades through the Pasig-Marikina River is runoff water from the slopes of Sierra Madre Mountains. Sierra Madre Mountains are mountain barriers in the eastern section of Luzon which stretch from the north to the south of the island. This area usually receives a very large amount of rainfall especially when there is a weather disturbance in the country. The highest mountain peak is about 1122 m, the lowest point is 28 m and the longest flow path is 42.85 kilometers. The land cover is dominated by shrubs with few percent covered by forest and natural grassland. Figure 2 shows the Pasig-Marikina River Basin extracted from SRTM elevation data and the river systems that drains to Laguna Lake and Manila Bay.

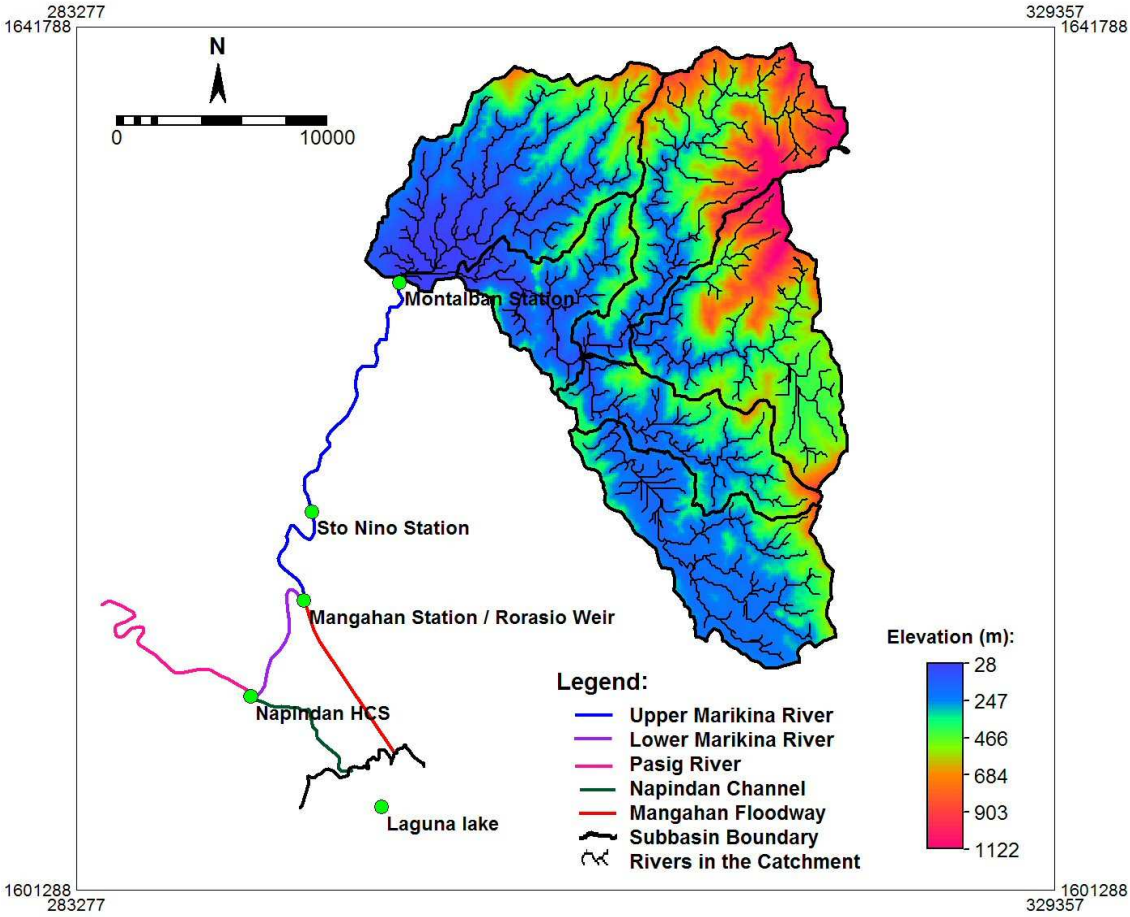

Figure 2: Pasig-Marikina River Basin and its river systems

Marikina River

The Marikina River is divided into two parts as shown in Figure 2; the upper Marikina River which is the stretch from Montalban water level gauging station down to the confluence of Mangahan Floodway (Mangahan station) and the lower Marikina River which runs from Mangahan station down to the confluence of Napindan channel. The total length of Marikina River is about 27 kilometers. The longitudinal profile of this river has a gentle slope up to Wawa Dam. A sharp slope can be seen from the Wawa Dam up to the Sierra Madre Mountains. Marikina River has a catchment area of 516.50 square kilometers at Napindan junction, 505.20 square kilometers at Rosario Weir, 465.20 square kilometers at Sto Nino water level gauging station and 377.82 square kilometers at Montalban water level gauging station.

Laguna Lake

The Laguna Lake is a large shallow lake with a maximum water depth of four meters. It serves as a natural retention reservoir to 21 subbasins comprising five provinces, including Metropolitan Manila basins. It has a surface area of approximately 900 square kilometers and 220 kilometers of shoreline. During flooding, the Laguna Lake, also called Laguna de Bay acts as the temporary storage of excess flood waters from Pasig and Marikina Rivers diverted through Mangahan Floodway and Napindan Channel. After the flood, flood water is flushed back to Pasig and Marikina Rivers using the same channels.

Mangahan Floodway

The Mangahan Floodway, built in 1986, is a nine kilometers artificial channel originally constructed to divert excess flood water from Marikina River to Laguna Lake. The average width of this channel is 220 meters. The design capacity of the channel is 2,400 cubic meters per second and is based on a 100 year return flood. The inflow to the floodway is controlled by the Rosario Weir consisting of eight gates located at Mangahan Floodway near the junction of the upper and lower Marikina River. Figure 3 shows the Rosario Weir with two gates open taken during the fieldwork campaign.

Figure 3: The Rosario Weir

The hydrometeorological conditions of Pasig-Marikina River Basin are being monitored through the telemetering system as shown in Figure 4. The Rosario Weir gates at Mangahan Floodway are opened whenever the water level in upper Marikina River reaches its threshold level so that it could not cause overflow flooding at the lower Marikina River and Pasig River which is mostly urban areas and vulnerable to flood. By opening the floodway gates, floodwaters will be diverted to Laguna Lake for temporary storage. When the water level at Pasig and Marikina River subsides, the stored water will be released back to Marikina River through Napindan channel. This channel connects the Laguna Lake to lower Marikina River.

However, during the implementation of the Effective Flood Control Operation System (EFCOS) Project, the Mangahan Floodway was redesigned to also accommodate the flushing out of water from Laguna Lake to Marikina River. The purpose of this is to mitigate flood damages in the coastline of the lake whenever the lake's water level is high.

Napindan Channel

Napindan Channel is a river that connects Laguna Lake to lower Marikina River. In the year 1983, The Napindan Hydraulic Control Structure (NHCS) was built at the mouth of Napindan Channel near the confluence of lower Marikina River. NHCS was originally designed to regulate salt water intrusion and polluted water from the Pasig River to enter the lake and to control the lake water level for the storage of water needed to ensure adequate supply for irrigation and other water needs around the area. However, due to increasing demand for a flood control system along Pasig-Marikina River, some modifications in Napindan Channel have been made.

Like the Mangahan Floodway, during the implementation of the EFCOS project, the NHCS was redesigned to drain flood water from Pasig and lower Marikina River to Laguna Lake when the water level of these rivers are high and allows flushing out of water from Laguna Lake to Pasig and lower Marikina River when the water level of the lake is high.

2.3. Mangahan Floodway Early Warning System

The Metropolitan Manila Development Authority (MMDA) through the EFCOS Project operates the Rosario Weir and NHCS and issues flood early warning in Mangahan Floodway whenever the Rosario Weir is opened. They have a network of telemetering system for rain gauges and water level stations within the basin.

EFCOS Project has been designed to protect the populated Metropolitan Manila areas along Pasig-Marikina River from overbank flooding by operating the Rosario Weir and NHCS. The main control point of its operation is the Sto Nino water level gauging station located at Marikina Bridge in Marikina City. Sto Nino water level gauging station was chosen as the control point because of the following reasons; Flood discharge is easily observed from the Marikina Bridge, the discharge is not affected by the operation of Rosario Weir and NHCS, and warning and gate operation is possible

during the flood travel time. It takes around 30 minutes for a flood wave to travel from Sto Nino water level gauging station to Rosario Weir (CTI Engineering Co. LTD., 1993).

During rainy season, usually from June to November or when there is a weather disturbance, EFCOS strictly follows the principle of flood operation. The flood operation requires the lowering of water level at Laguna Lake before the actual flooding occurs. This is done to create extra storage capacity once the flood occurs. The procedure is discussed in Appendix C.

EFCOS has classified flood phase into four as indicated in Appendix B. Flood phase starts at Precaution Stage. This is when the water level at Sto Nino water level gauging station is more than 13.0 m which corresponds to approximately 150 m^3/s. Usually, during this stage, all gates of Rosario Weir are closed and "Announcement A" is given to all persons within the floodway channel as a precautionary measure.

The Caution Stage follows when the water level at the control point is still increasing. This time, some gates are opened causing abrupt flow surge in the floodway channel. A warning consisting of siren warning, speaker warning and "Announcement B" is issued thirty minutes before the gates open. During Emergency Stage, "Announcement C" and speaker warnings are broadcasted. The Post Flood Stage follows the Emergency Stage and "Announcement D" is broadcasted.

The flood warning system is only designed for the Mangahan floodway. There are nine warning posts along the left and right banks equipped with voice warnings and sirens as shown in Figure 4. Script of the voice warnings is attached as Appendix D. During normal conditions, the warning is audible up to 1.5 kilometers and up to 1.0 kilometer when there is an inclement weather. The warning posts are operated at the master control station near the Rosario Weir. On the average, the Rosario Weir is opened for flood control management six to ten times a year.

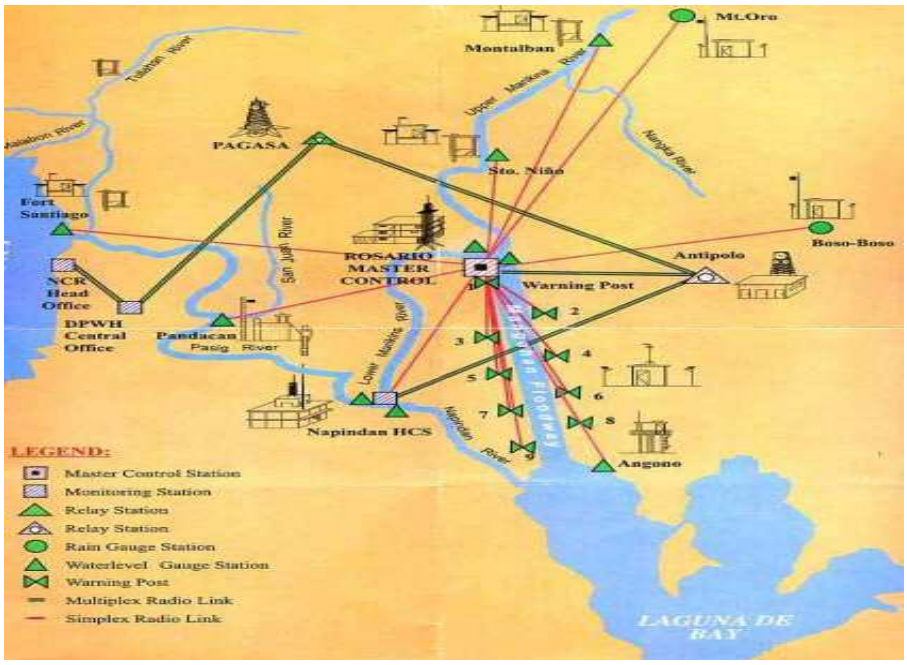

Figure 4: EFCOS telemetry and warning systems
Source: JBIC (2001)

2.4. Weather and Climate

The climate of the Philippines is tropical and maritime. It is characterized by relatively high temperature, high humidity and abundant rainfall (PAGASA, 2004). The annual average temperature is 26.6°C. The coldest month is January with an average temperature of 25.5°C and the warmest is May with an average temperature of 28.3°C. There is no significant difference on average temperature for the whole country despite having a wide range of latitude. Humidity varies between 71 percent in March to 85 percent in September.

The classification of climate in the Philippines is based on rainfall distribution. Figure 5 shows the types of climate and its description. Rainfall is considered to be the most important climatic element in the Philippines. Distribution of rainfall throughout the country varies from one region to another. The country's mean annual rainfall varies from 965 to 4065 millimeters.

The Pasig-Marikina River Basin has a Type I climate. The annual rainfall for this basin ranges from 1700 to 3200 millimeters per year. About 80 percent of the annual rainfall occurs during rainy season. The year round distribution of rainfall is influenced by the weather systems that affect the river basin. Tropical cyclones and southwest monsoons are the main rain-bearing weather systems that affect the catchment and they occur during the months of July to November. Serious flooding usually occurs from August to November.

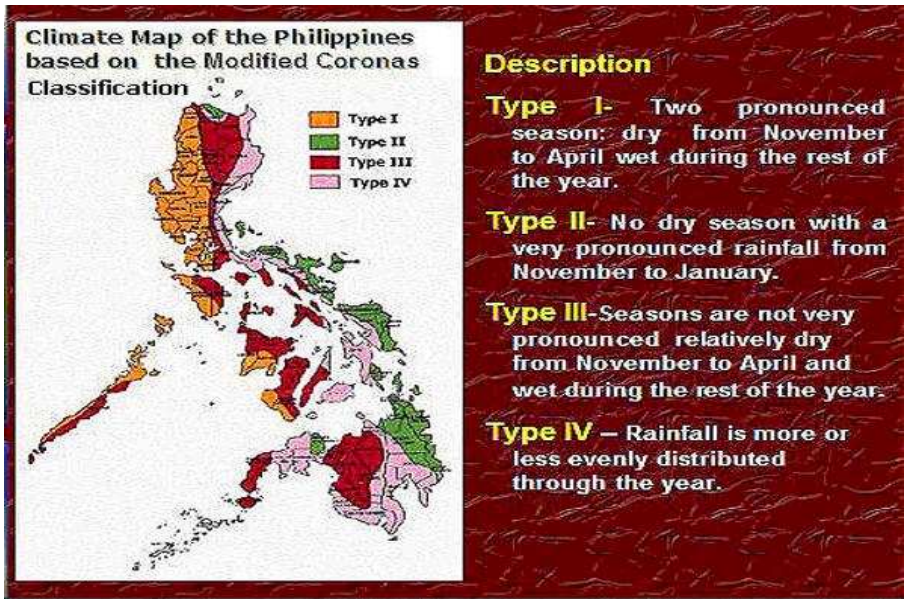

Figure 5: Climate of the Philippines
Source: PAGASA (2004)

2.5. Topography

The Pasig-Marikina River Basin is located east of Metropolitan Manila and bounded by the provinces of Bulacan in the north, Quezon in the east and Laguna in the south. The basin's topography is characterized by a combination of valleys and mountains. The flat and low lying areas are located on the western section of the river basin while gentle rolling hills and some rugged ridges are on the

eastern section. These rugged ridges form part of the Sierra Madre Mountains which extends along the eastern stretch of Luzon Island with a highest elevation of about 1122 meters above mean sea level.

2.6. Problem Statement

Metropolitan Manila has been experiencing severe flooding since time immemorial. One of the main causes of flooding in this area is the big river discharge from Marikina River. This river drains flood waters from Pasig-Marikina River Basin. The cities and municipalities along Pasig and Marikina Rivers experiences floods of different magnitudes following heavy rain pour in Pasig-Marikina River Basin.

To overcome this recurrent flooding problem, combined structural and non-structural mitigation measures were implemented in Marikina River. Among the first project to be completed was the Mangahan Floodway. As discussed in section 2.2, Mangahan Floodway serves as a diversion canal when water level in Marikina River rises above a defined threshold value. This is done by opening the sluice gates at Rosario Weir located at the mouth of Mangahan Floodway near the confluence of Marikina River.

Figure 6 shows the current situation at the banks and slopes of Mangahan Floodway. Residential and small commercial buildings were built along the floodway banks which could be dangerous whenever Rosario Weir is opened without flood early warning system. There are also some residents who go fishing on the floodway. Presently, there is no hydrological model for Marikina River that could be used as basis for the operation of Rosario Weir and NHCS. This research will try to address this problem by developing a hydrologic model in Pasig-Marikina River Basin and a hydraulic flow model along upper Marikina River.

Figure 6: Part of Mangahan Floodway showing informal settlers on the side slopes of the floodway
Source: Google Earth (2007)

This study will focus on the development of a hydrological models that could be used as basis for the operation of EFCOS' Rosario Weir and NHCS for their flood control and early warning activities. The HBV semi-distributed model will be calibrated and used to simulate the river discharge in Pasig-Marikina River Basin down to Montalban water level gauging station. Montalban water level gauging station is the uppermost water level gauging station of Marikina River. From there, the DUFLOW model will be used to simulate the flood wave propagation down to Mangahan station near the confluence of Mangahan Floodway.

2.7. Research Objectives

2.7.1. General

- To develop a HBV model for Pasig-Marikina River Basin and a DULOW model for the upper Marikina River. The calibrated models could be used by EFCOS as basis for the operation of Rosario Weir in Mangahan Floodway and Napindan Hydraulic Control Structure in Napindan Channel for its flood control and early warning operations.

2.7.2. Specifics

- To extract hydrological parameters from SRTM DEM.
- To calibrate and validate HBV model in Pasig-Marikina River Basin using hourly hydrometeorological data.
- To use DUFLOW model along upper Marikina River to simulate the flood propagation.

2.7.3. Research Questions

- How accurate can the HBV semi-distributed model simulate the discharge at Montalban water level gauging station?
- Can a DUFLOW model simulate accurately the flood wave propagation along upper Marikina River?
- How does the runoff hydrograph changes along the channel network?
- How to extract HBV semi-distributed model inputs from SRTM DEM?
- What is the flood lag time from Pasig-Marikina River Basin to Sto Nino water level gauging station?

3. Literature Survey

3.1. Hydrologic Cycle at Catchment Scale

At a catchment scale, considerations of hydrological cycle include the processes that take place in the atmosphere, land surface and subsurface as illustrated in Figure 7. The precipitation falls from the atmosphere but before it reaches the ground, part of it is intercepted by vegetation and evaporates back into the atmosphere. The precipitation that reaches the land surface will either infiltrate to the subsurface or will become Horton overland flow or rill flow. As the rill flow accumulates, it becomes a stream flow then channel flow. Channel flow also has some contribution from the groundwater flow in the form of baseflow. It becomes the catchment runoff when it flows out from the catchment.

Rainwater that infiltrates will contribute to unsaturated flow, macro pore flow and perched flow. Unsaturated flow will recharge the groundwater through the process of percolation. Water that passes through macro pore and perched flow will either contribute to the groundwater flow or to the exfiltration process depending on the soil moisture condition. When rainwater reaches the groundwater through percolation, part of it will join the channel flow as baseflow and again evaporation will take place. Majority of the groundwater will remain as groundwater recharge or groundwater storage. The total evaporation is the summation of the canopy evaporation, transpiration and soil evaporation and evaporation from open water. The catchment runoff is the accumulation of the channel flow and the contribution from the groundwater.

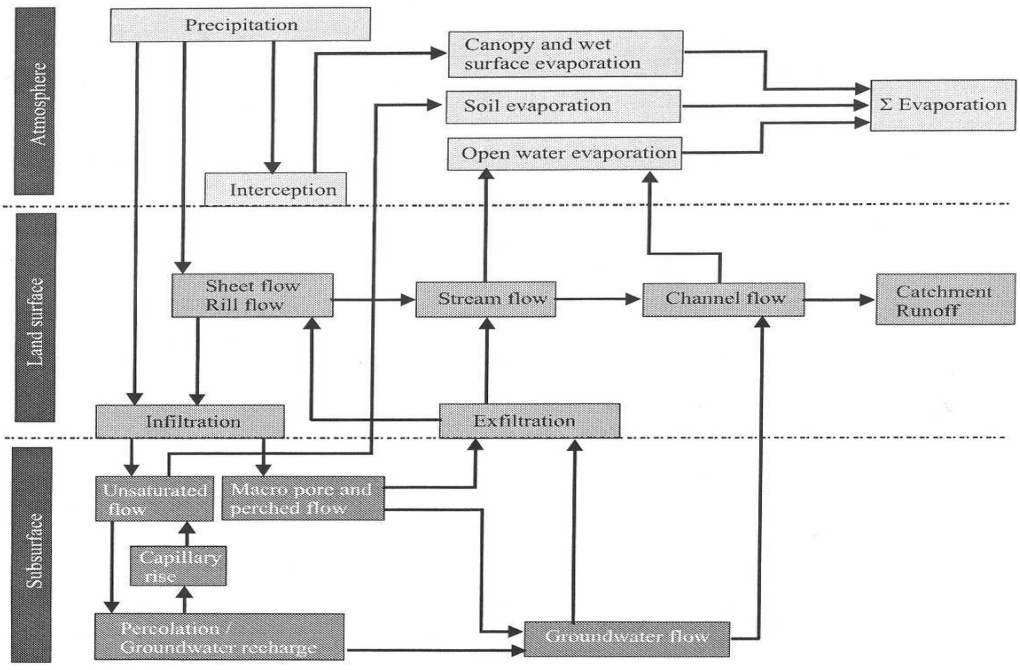

Figure 7: Major processes of the schematized hydrologic cycle at a catchment scale
Source: Rientjes (2007)

3.2. Runoff Processes

Runoff from a catchment is often expressed by a river flow hydrograph. The shape of a river flow hydrograph in a particular catchment is a combined function of physiographic characteristics of the catchment and the meteorological variables (Bedient et al., 1988). Physiographic factors that affect the flow in a catchment includes; size and shape of the catchment, slope of the river system and the storage capacity of the catchment. Meteorological factors includes; rainfall intensity, duration and distribution over the catchment and evaporation. Figure 8 illustrates the runoff processes in a sloping area in a catchment scale.

During storm, when the intensity of rain is higher than the soil infiltration capacity, a process known as Horton overland flow occurs. This flow can be seen as a thin layer sheet that flows overland. Saturated overland flow occurs when the soil becomes saturated because of groundwater level rise. This phenomenon is mostly observed at the foot of the hills or mountains with shallow groundwater level. The Unsaturated subsurface flow occurs when there is infiltration. This flow is mostly characterised by its vertical flow and can be in the form of either matrix flow or macro pore flow. The movement of water in unsaturated subsurface flow is mainly caused by suction head gradients. Perched subsurface flow is mostly observed in the flow of water in the matrix wherein the saturated hydraulic conductivity of a given subsurface is much lower than the overlying layer.

Another type of flow that occurs in the subsurface is the macro pore flow. This flow is observed in the small pores created by worms, vegetation roots and soil cracks. The most important characteristic of macro pore flow is that it is not controlled by suction heads. Groundwater flow is considered as the flow of water in the saturated zone. All of the percolated water is stored here. Groundwater flow is characterized by its large storage volume and low system dynamics compared to other flow processes and it contributes to the baseflow component of the hydrograph in either rapid or delayed fashion. Water will finally reach the natural or artificial drainage system and will be transported through channel flow.

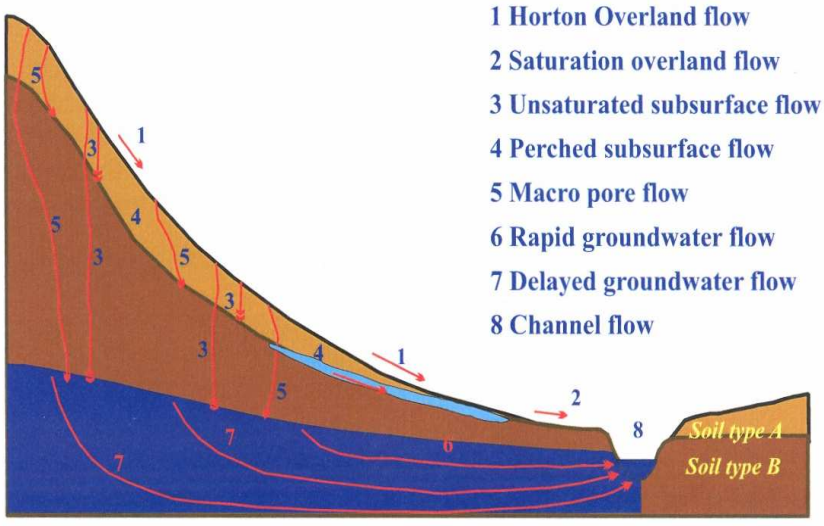

Figure 8: Schematization of runoff processes in a sloping area at a catchment scale
Source: Rientjes (2007)

3.3. Hydrologic and Hydraulic Modelling

Hydrologic Modelling

A hydrologic model is a mathematical representation of hydrological processes in a catchment in a simplified form. It can be used to better understand and explain hydrological processes and for hydrologic prediction (Haan et al., 1982). There are two different types of hydrologic models depending on the model approach that are deterministic and stochastic models. Deterministic models are based on the physical processes in the catchment it is representing. A model can be called as deterministic model if it does not consider randomness, meaning, specific input will always have the same output (Chow et al., 1988). Stochastic models on the other hand refer to models which deal with random variables. These variables have a probability of distribution in parameter space (Rientjes, 2007). The main application of a hydrologic model is to simulate river discharge in a catchment. Hydrologic models are increasingly used in water resources management and applications range from simple planning of water resources to more complex issues like assessing effects of climate change on water resources and environmental issues. Models are also used in studying the interaction between surface water and groundwater. Another application of hydrologic models is in flood forecasting and early warning.

Hydrologic models vary from simple lumped models to semi-distributed models and to more complex distributed models. Moreover, applications of these models in water resources vary from event based modelling to water balance modelling and to continuous stream flow modelling. The number of parameters and state variables needed to calibrate a model may differ depending on the model type and complexity. Physically based distributed models need enormous amount of data which is difficult to obtain especially in remote areas. However, with the advent of remote sensing and geographic information system, data in those areas can now be obtained.

Hydraulic Modelling

In hydraulic modelling, flow in the channel is simulated by solving the complete set of St. Venant equations, first derived in 1871. This type of model is based on continuity equation (conservation of mass) and momentum equation (conservation of momentum). These equations are solved numerically by either explicit or implicit methods (Bedient et al., 1988). The explicit method solves the velocity and depth in a particular point in the river using the previously known data only. The implicit method solves the equations simultaneously at each time step and over all calculation points that cover the entire river. In order to derive the Saint Venant equations, the following assumptions are often made (Chow et al., 1988):

1. The flow is one-dimensional; depth and velocity vary only in the longitudinal direction of the channel. This implies that the velocity is constant and the water surface is horizontal across any section perpendicular to the longitudinal axis.
2. Flow is assumed to vary gradually along the channel so that hydrostatic pressure prevails and vertical accelerations can be neglected.
3. The longitudinal axis of the channel is approximated as a straight line.

4. The bottom slope of the channel is small and the channel bed is fixed; that is, the effect of scour and deposition are negligible.
5. Resistance coefficients for steady uniform turbulent flow are applicable so that relationships such as Manning's equation can be used to describe resistance effects.
6. The fluid is incompressible and of constant density throughout the flow.

Usually, hydraulic models are used to simulate movement of flood waters along the waterways, storage elements and hydraulic structures. These types of models can simulate the flood levels and flow patterns and can model the complex effects of backwater or tidal intrusion, overtopping of embankments, waterways confluences and diversions, bridge constrictions, weirs, culverts and pumps and other obstructions on the flow in the river system. Because of its capabilities, hydraulic models became an important tool in river basin management around the globe.

3.4. Flood Modelling

Due to the damages brought by floods to our society as discussed in section 1.1, flood models have become an indispensable tool in flood management. Flood models can either be used in planning and design, land use zoning or flood forecasting. Government authorities usually use flood models in determining flood hazard zones and flood extent in their locality. For this purpose, two dimensional flood models are mostly used. This type of model requires a detailed digital elevation model of the area including; building footprints, roads and bridges, sewer systems and others that will affect the flow of water.

Most of the applications of flood models are on the operational flood forecasting and early warning systems. Data requirement for this type of model includes; digital elevation model (DEM), river network and cross sections, surface roughness coefficient, land cover and land use maps and river stage or discharge data. If there are hydraulic structures along the river, time series data of its operation must also be known.

Calibration of hydrological model varies on its application. Models used for flood forecasting and early warning systems are optimized to fit the peak and the time of peak. These are two of the most important flood wave characteristics that a flood model must be able to predict accurately. Also, operational flood forecasting models will not be effective if there is no reliable real time hydrometeorological data. Present day technology enables the collection of much needed data through automated systems. Another factor that determines the effectiveness of a flood forecasting and warning system is the lag time. This is the length of time for a drop of rain to travel from the catchment to the forecasting point. Usually, lag time is utilized for emergency response and evacuation. If the lag time is shorter than the preparation time, as in the case of flash flooding rivers, ordinary flood models will not be useful. In this case, more advanced flood models that utilize forecasted rainfall will be more effective. Haan et al. (1982) proposed four factors that can be used in selecting appropriate model; accuracy of prediction, simplicity of the model, consistency of parameter estimates and sensitivity of results to changes in parameter values.

3.5. Remote Sensing and Geographic Information System in Flood Modelling

Remote sensing is the process of gathering catchment information and hydrologic state variables through the use of measured electromagnetic spectrum (Maidment, 1993). In remote sensing, electromagnetic energy is measured through the use of sensors. Sensors used in remote sensing are carried by platforms with altitude ranging from few centimetres (e.g. handheld field equipment) up to orbits in space of thousands of kilometers (e.g. geostationary satellites) and beyond (Janssen et al., 2001). The sensors that are used for hydrological applications can either be passive or active and it covers a broad range of the electromagnetic spectrum. Data acquired through remote sensing tremendously trigger advancements in flood modelling. During the early days of flood modelling, data acquisition was the major limitation for its advancement. Data acquisition activity is often considered the most time consuming and costly component in flood modelling.

Aside from the catchment information that can be derived from remote sensing data, another break through in remote sensing technology was the development of rainfall estimation algorithms. Rainfall estimation techniques started using the visible and infrared channels and its combination (e.g. bispectral algorithm). Some algorithms that use visible sensors assume that raining clouds appears brighter than the non-raining clouds. Cloud top temperatures are the basis for the algorithms that uses the infrared channels. Advanced rainfall estimation algorithms used a more accurate sensor, radar. Precipitation Radar (PR) onboard the Tropical Rainfall Measuring Mission (TRMM) was the first space borne instrument to provide a three dimensional storm structure (NASA, 2006). Using the products of these advanced technologies, estimated rainfall information can now be entered to a flood model thereby increasing the flood lead time.

Another technology advancement that benefited flood modelling is the development of Geographic Information System. Geographic Information System (GIS) is a system that facilitates the preparation and analysis of georeferenced data (de By et al., 1999). Burrough (1986) defined GIS as a tool that can be used in coding, storing and retrieving geographic information. The above definitions suggest that with the use of GIS, data handling and pre-processing in flood modelling can be done systematically and accurately. GIS can put together geographic information from different sources thereby maximizing the analytical power of the model.

Integrating the capabilities of remote sensing and geographic information system has tremendously improved flood modelling. It enables to model in a distributed fashion the topographic parameters and variables even in large scale hydrologic systems. Digital Elevation Model (DEM) extraction from remotely sensed data (e.g. SRTM elevation data) is nowadays most common. From the DEM, the basin boundary, drainage network, area and elevation can be extracted using GIS applications. Other examples of remotely sensed data that can be processed using GIS includes the spatial distribution of land cover, land use and soil characteristics.

Table 2: Some spectral bands used in remote sensing and its principal applications

Band (μm)	Applications
Visible Blue (0.45-0.52)	Water characteristics, water depth, soil and vegetation discrimination, forest-type mapping and geology.
Visible Green (0.52-0.60)	Vegetation discrimination and vigor assessment, analysis of cultural features and urban infrastructure, and water quality studies (nutrient load)
Visible Red (0.63 – 0.69)	Vegetation discrimination, assessing plant condition, delineating soil and geologic boundaries and identifying cultural features.
Near Infrared (0.70-1.0)	Vegetation mapping, crop-condition monitoring, biomass estimation, soil moisture assessment and delineating water features.
Short-wave Infrared (1.0-3.0)	Land-cover classification, vegetation analysis, moisture levels in soil, monitoring plant vigor and crop condition, cloud-snow-ice discrimination.
Medium-wave (3.0-8.0) and Long-wave Infrared (8.0-14.0)	Measuring temperature of feature, detecting thermal features, vegetation stress, soil moisture and geology.

Source: Aronoff (2005)

3.6. Previous Study in the Area

The Pasig-Marikina River Basin, even though considered as the main source of flood waters in the low lying areas along the Pasig-Marikina River requires more study. Most studies conducted in the area are about water quality and for the downstream part of Pasig-Marikina River. Research by Madsen et al. (2006) deals with the flood forecasting and warning operations. Madsen et al. (2006) executed research on adaptive state updating in real-time river flow forecasting in the study area using MIKE 11 channel flow model. The updating technique they used was based on an explicit description of Kalman gain vector using pre-defined functions in describing the spatial distribution of model errors. The EFCOS, which is the implementing agency, employed the model but only managed to use it for one year because of technical problems.

4. Materials and Methodology

4.1. General Methodology

This research follows the general methodology that is shown by the flowchart in Figure 9. Two models were used for this research; the HBV semi-distributed model and the DUFLOW model. The setup for each model is described in section 4.2 and 4.3, respectively.

After fieldwork campaign, the databases for each model were prepared and checked for inconsistencies. Next, the HBV model was setup, calibrated and validated. After the HBV model calibration, the DUFLOW model was setup and calibrated using the Montalban station data as the upstream boundary condition and the Mangahan station data as the downstream boundary condition. The DUFLOW model was calibrated at Sto Nino water level station and the RAM module was used to simulate the lateral inflows for the area between the upstream boundary (Montalban station) and the calibration point (Sto Nino station). After DUFLOW calibration, the channel flow hydrograph of the HBV model was entered to the DUFLOW model as the upstream boundary condition but the downstream boundary condition remains the same.

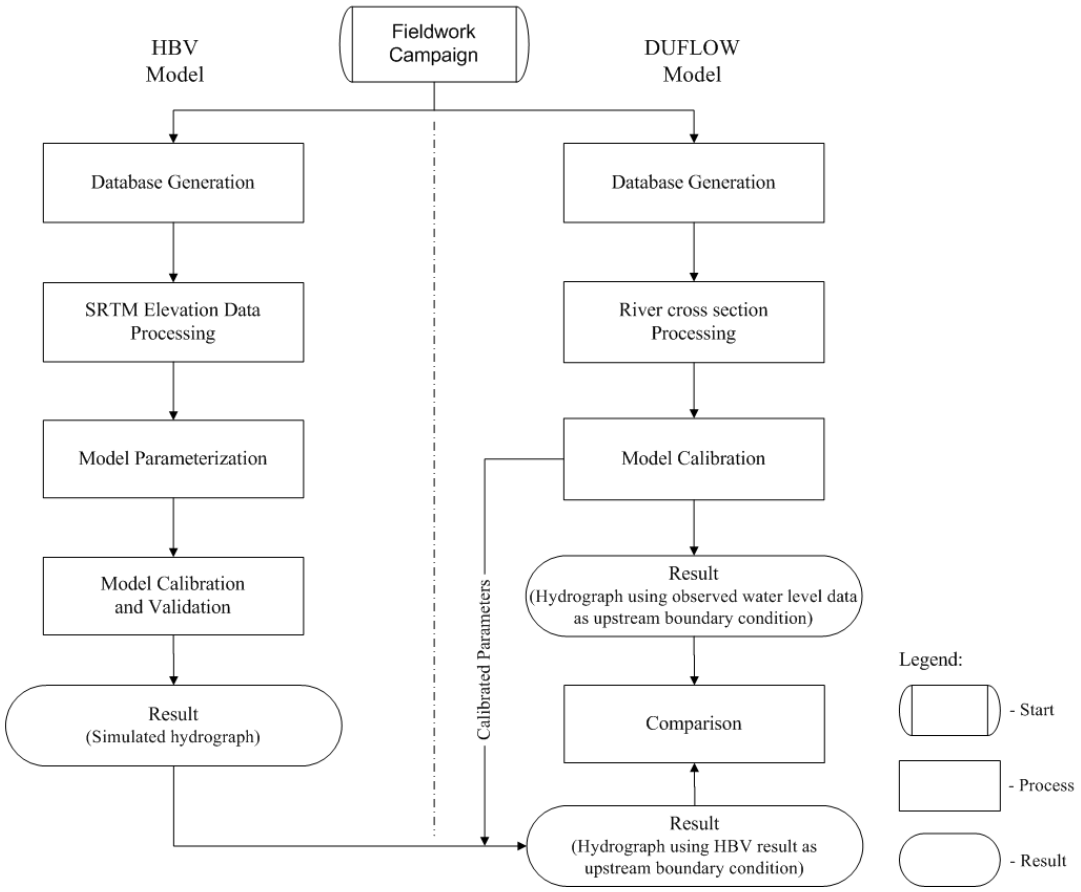

Figure 9: General methodology flowchart

4.2. HBV Model

4.2.1. Model Background

HBV is a conceptual hydrological model mostly used for the simulation of continuous runoff. This model was originally developed at the Swedish Meteorological and Hydrological Institute (SMHI) in the early 70's with the purpose of assisting hydropower operations. The role of HBV in hydropower operations during that time was limited to providing hydrological forecast for planning purposes (SMHI, 2006). The model name HBV came from the acronym of Hydrologiska Byråns Vattenbalansavdelning (Hydrological Bureau Waterbalance) which was a section of SMHI. The operational forecast was first applied in the northern part of Sweden in 1975. From then on, HBV model has been used in over 40 countries around the globe for operational and scientific applications. The HBV model routines had undergone a comprehensive re-evaluation in the early 1990's and resulted in the HBV-96 version. This model serves now as the standard tool used by the national warning service in Sweden. Figure 10 shows the schematic diagram of the HBV model. The summary of the HBV model was obtained from IHMS manual version 5.10.

The basic modelling philosophy behind the model is (Lindstrom et al., 1997):

- The model shall be based on a sound scientific foundation;
- Data demands must be met in typical basins;
- The model complexity must be justified by model performance;
- The model must be properly validated;
- The model must be understandable by users.

4.2.2. Model Structure

The HBV model (Bergstrom, 1976, 1992) is a rainfall-runoff model which includes conceptual descriptions of hydrological processes at the catchment scale. The model structure consists of a precipitation routine, a soil moisture routine, a response function and a routing routine. The model also includes routines to handle regulations. The input data includes precipitation records on daily or shorter time step, air temperature records if snow is present, monthly estimates of evapotranspiration and runoff records for calibration. HBV model was developed and tested on basins with an area of 40 square kilometers, but can be used to simulate river flow of any other area (Lindstrom et al., 1997).

The HBV model has the capabilities of a semi-distributed model. This means that a river basin can be divided into sub-basins, which in turn can be divided into different vegetation zones, usually forest and open lands, and lake areas (Andersson et al., 2006). The model was originally developed using daily time steps but some research (e.g. Kobold et al., 2006) proved that this model can also be used using hourly time steps.

The present version of HBV model is an Integrated Hydrological Modelling System (IHMS): a modern, well tested and operational tool. HBV has the capabilities of linking with real time Weather

Information and Forecasting System, such as the WebHyPro system developed by SMHI (SMHI, 2006). In IHMS, aside from the HBV model, useful functionalities were added such as; database management, presentations and various tools for hydrological forecasting and statistical analyses.

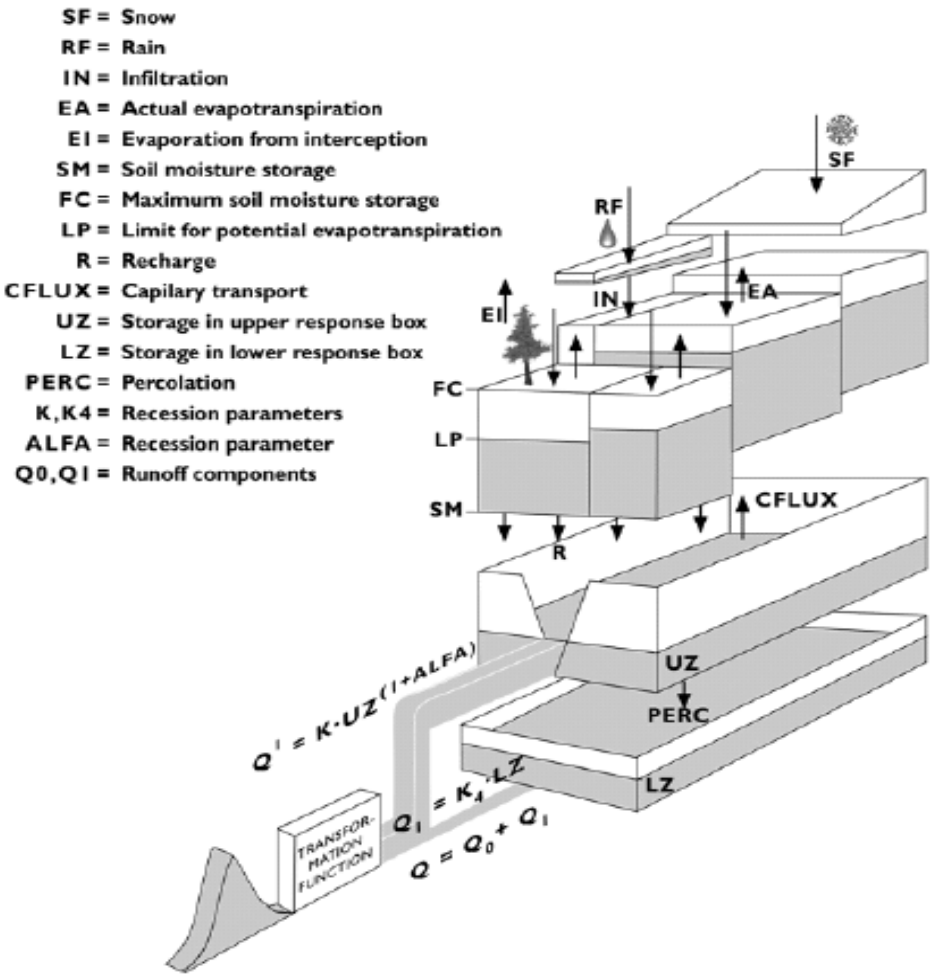

Figure 10: Schematic diagram of HBV-96 model structure
Source: SMHI (2006)

The general water balance equation used in HBV:

$$P - E - Q = \frac{d}{dt}\left[SP + SM + UZ + LZ + LAKES\right] \qquad [1]$$

where;

P	= Precipitation
E	= Evapotranspiration
Q	= Runoff
SP	= Snow pack
SM	= Soil moisture
UZ	= Upper groundwater zone
LZ	= Lower groundwater zone
$LAKES$	= Lake volume

4.2.3. Model Routines

Precipitation and Snow Accumulation

Precipitation is the main meteorological forcing term of runoff in a catchment. In HBV, it is simulated either as a snow or rain depending on the threshold temperature *tt* (degrees Celsius) and the actual air temperature *T* (degrees Celsius). If the actual air temperature is higher than the threshold temperature, precipitation is considered rain.

The standard snowmelt routine used in HBV model is a degree-day approach. This is based on air temperature and the water holding capacity of snow which delays runoff. Snow melt is further modelled according to the temperature lapse rate. Forest and open areas are also modelled differently (Lindstrom et al., 1997).

Soil Moisture

The soil moisture accounting routine is the main part that controls runoff formation. This routine has three parameters; *Beta*, *LP* and *FC*. *Beta* is the exponential term which controls the contribution of precipitation into the response function ($\Delta Q/\Delta P$) as shown in equation [2]. *SM* in equation [2] is the computed soil moisture storage and *FC* is the maximum soil moisture storage. The term ΔQ is often called the effective precipitation and $\Delta Q/\Delta P$ is the runoff coefficient. Soil parameter *LP* is the soil moisture value above which evapotranspiration reaches its potential value. The value of parameter *LP* is given as a fraction of *FC*. The effect of soil moisture routine in the model is that the precipitation contribution to the runoff is small when the soil is dry and large when the soil is wet. Proper soil moisture accounting plays a vital role in hydrological modelling and is proven to be very effective and is relatively not sensitive to scales (Bergstrom et al., 1998).

$$\frac{\Delta Q}{\Delta P} = \left(\frac{SM}{FC} \right)^{\beta eta} \qquad [2]$$

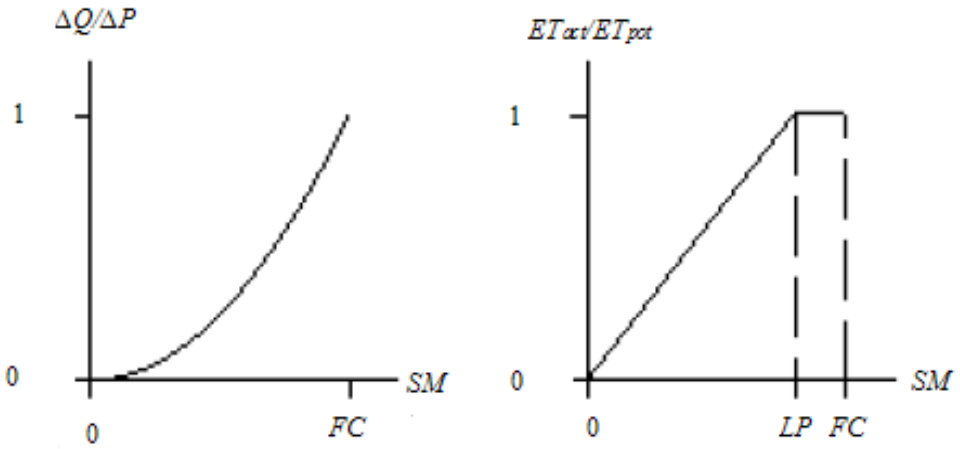

Figure 11: Schematization of soil moisture parameters

Response Routine

The response function transforms the excess water from the soil moisture zone to runoff. This routine controls the dynamics of the generated runoff. Also, this routine accounts for the direct effect of precipitation and evaporation on lakes, rivers and other wet areas. Response function has two components; the upper, non linear reservoir and the lower, linear reservoir. The upper and the lower reservoirs are sources of the quick and slow runoff components of the hydrograph, respectively.

The effective rainfall, ΔQ, will be added to the storage in the upper reservoir. As long as water is present in the upper reservoir, water will continuously percolate to the lower reservoir according to parameter *Perc*. If there is a high yield from the soil and percolation is not adequate to empty the upper reservoir, part of the generated discharge will come directly from the upper reservoir which represents drainage through more superficial channels. Equation [3] is used in simulating the outflow from the upper reservoir, Q_0 (mm). The parameter *Alfa* is a measure of the non linearity and has a value range between 0.5 to 1.1. *UZ* (mm) is the upper reservoir content and *K* is the recession coefficient. Parameters used in computing for the value of *K* are; *Khq*, *Hq* and *Alfa*. *Hq* is a high flow level at which the recession rate *Khq* is assumed. The value of *Hq* can be computed using equation [5], where; *Mq* (m^3/s) is the mean of the observed discharge, *Mhq* (m^3/s) is the mean of annual peaks and *A* (sq. km) is the catchment area. The yield from the lower reservoir Q_1 (mm) is given in equation [4], where; *LZ* (mm) is the lower reservoir content and *K4* is the recession coefficient.

$$Q_0 = K \cdot UZ^{(1+alfa)} \quad [3]$$

$$Q_1 = K4 \cdot LZ \quad [4]$$

$$Hq = \frac{86.4\sqrt{Mq \cdot Mhq}}{A} \quad [5]$$

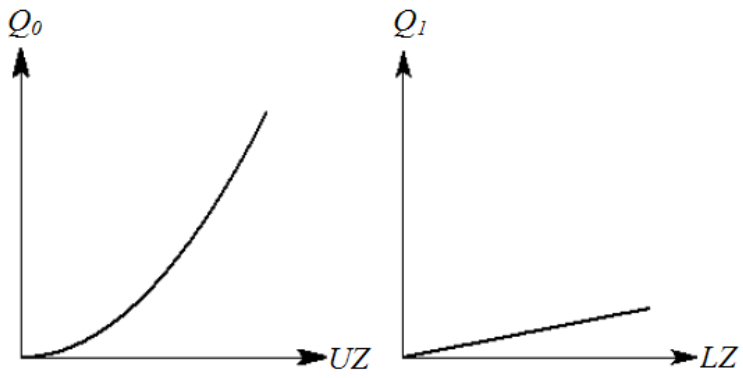

Figure 12: Schematization of the outflow from upper and lower reservoirs

Transformation Function

The generated runoff from the dynamic part of the model is routed through a transformation function. The purpose of this routine is to get the proper shape of the hydrograph at the outlet. HBV's

transformation function is composed of a simple filtering technique with a triangular distribution of weights as shown in Figure 13. The time base with a triangular distribution is handled by the parameter *Maxbaz*. HBV's routing process is simulated using a modified Muskingum approach.

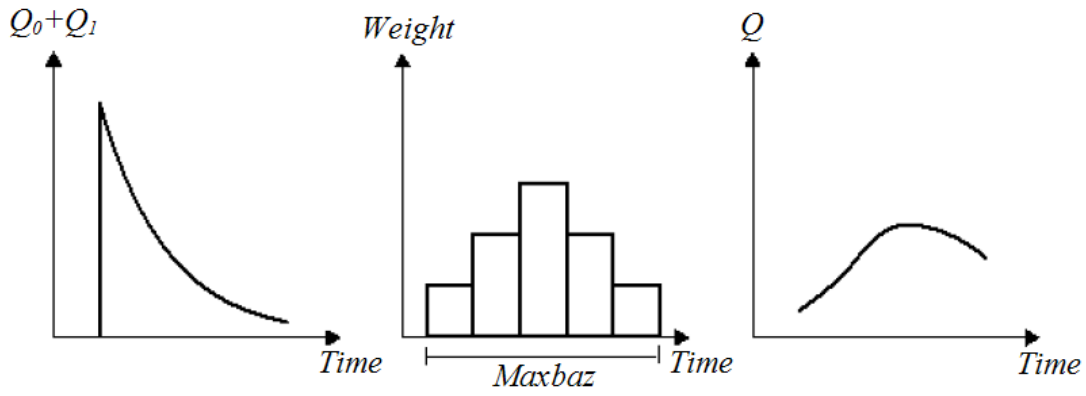

Figure 13: Schematization of transformation function parameters

4.2.4. Model Calibration

The calibration of HBV-96 model can be done by fine tuning the parameters. There are three parameters involved in the soil moisture routine; *FC* which is the maximum soil moisture storage, *LP* which is the soil moisture value above which ET_{act} reaches ET_{pot} and *Beta* which is the parameter that determines the relative contribution to the runoff from precipitation. The soil moisture parameters control the water balance of the model and have a direct effect on the baseflow. The response function routine has three parameters; the *Alfa*, *Khq* and *Hq*. All of these parameters have an effect on the shape of the hydrograph and the peak discharge.

The goodness of fit of the simulated to the observed runoff can be assessed by three different criteria; Visual interpretation of plots for observed and simulated runoff, continues plot of the accumulated difference which is represented by equation [6];

$$Accdiff = \sum (Q_{sim} - Q_{obs}) * C_t \qquad [6]$$

where;

Q_{sim} = Simulated discharge

Q_{obs} = Observed discharge

C = Coefficient transforming to mm over the basin

t = Time

and the Nash-Sutcliffe model efficiency coefficient (Nash et al., 1970) which is mostly used to assess the predictive power of a hydrological model. The Nash-Sutcliffe efficiency coefficient is shown in equation [7];

$$R^2 = 1 - \frac{\sum_{i=1}^{n}[Q_{sim}(i) - Q_{obs}(i)]^2}{\sum_{i=1}^{n}(Q_{obs}(i) - \overline{Q_{obs}})^2} \quad [7]$$

where;

Q_{sim} = Simulated discharge

Q_{obs} = Observed discharge

The value of Nash-Sutcliffe efficiency coefficient (R^2) varies form -∞ to 1. R^2 value of 1 indicates that there is a perfect match between the observed and the simulated data. However, R^2 =1 is seldom achieved in actual calibration. R^2 =0 means that the prediction capabilities of the model is just equal to the mean of the observed data, while R^2 <0 indicates that the observed mean can predict better than the model.

4.2.5. Model Setup

The semi-distributed version of HBV model was used for this study. This model was set up using hourly hydrometeorological data. Input data required for this model are rainfall, air temperature, potential evapotranspiration and land cover. Discharge at the outlet of the catchment was also needed for calibration and validation. SRTM elevation data of the area was also used for this study and the evapotranspiration was computed using the Penman-Monteith method.

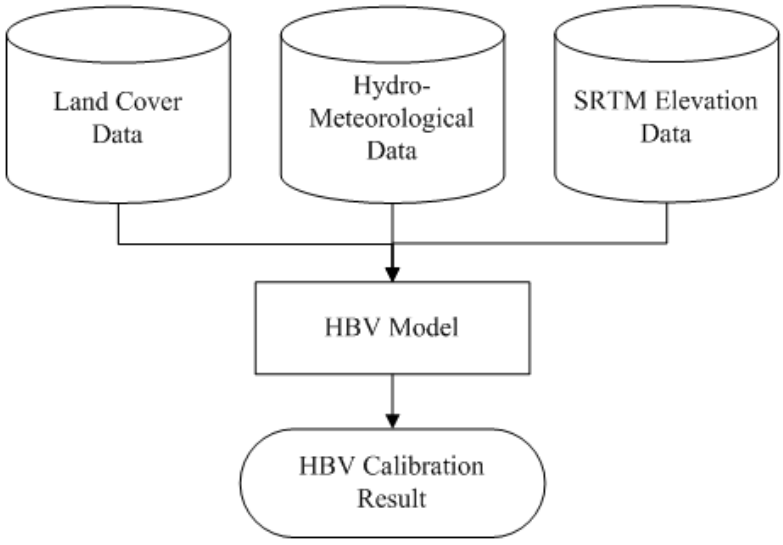

Figure 14: Schematization of model input/output in the HBV model

The modelled domain which is approximately 377.82 square kilometers was divided into six subbasins as shown in Figure 15. This figure also shows the river systems in the catchment. Subbasin areas are shown in Table 3. Land cover in each subbasin was derived from the land cover map. The HBV model requires forest, field, lake and glacier land cover types. However, for the study area, only

the forest and field are applicable. Since the original land cover map has several land cover types, it was reclassified to match the model input requirement.

Table 3: Subbasin areas used in the HBV model

Subbasin Name	Area (km^2)
Subbasin1	64.01
Subbasin2	73.65
Subbasin3	41.07
Subbasin4	77.22
Subbasin5	35.02
Subbasin6	86.85
Total Basin Area	377.82

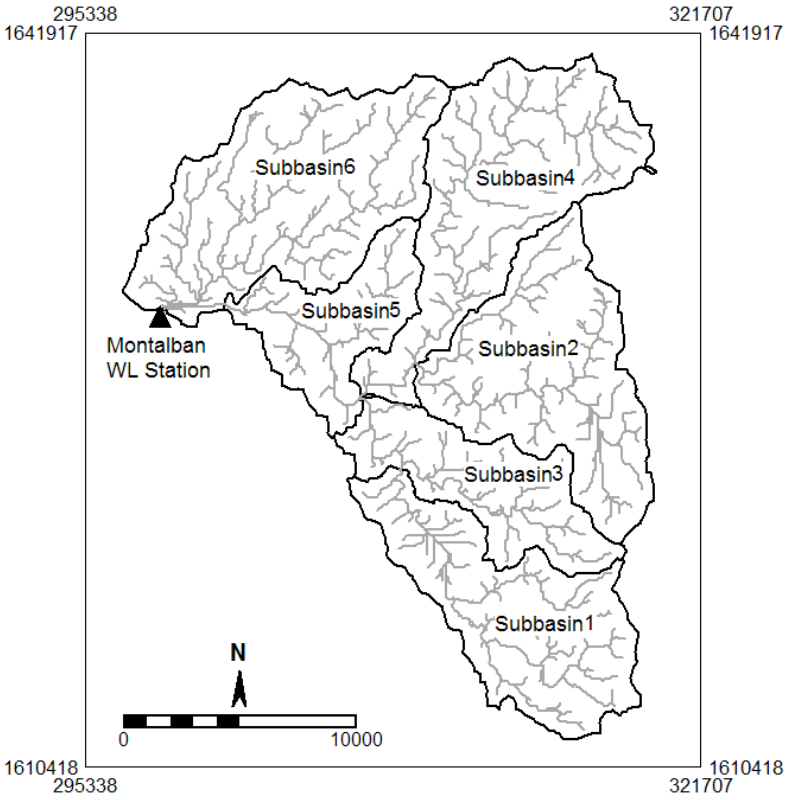

Figure 15: Pasig-Marikina River Basin divided into different subbasins

Figure 19 shows the land cover map and Table 4 shows the area covered by each land cover per subbasin. Each land cover in every subbasin was sliced and grouped at 100 meters elevation difference. The reason is that the correction in rainfall for altitude is based on 100 meters elevation difference.

Table 4: Land cover zones and areas in each subbasin

Subbasin Name	Land Cover		Total Area (km^2)
	Field (km^2)	Forest (km^2)	
Subbasin1	63.79	0.22	64.01
Subbasin2	53.79	19.86	73.65
Subbasin3	40.31	0.76	41.07
Subbasin4	30.61	46.61	77.22
Subbasin5	35.02	0	35.02
Subbasin6	79.16	7.69	86.85

The contribution of each rainfall station to subbasins was determined by inverse distance weighted interpolation method. This method was chosen because it takes into account the rainfall contribution of every rainfall station. A rainfall station nearer to the interpolated point has a greater weight compared to a station which is at large distance. For this study however, only the center of the subbasin was considered in the interpolation. The weight derived using the center of the subbasin was applied to the whole subbasin. The power parameter (p) used for this study was 2. Table 5 shows the computed weights of each rainfall station in every subbasin. Also, equation [8] shows the inverse distance weighted interpolation equation used in deriving weights.

$$w_i = \frac{h_i^{-p}}{\sum_{j=1}^{n} h_j^{-p}} \qquad [8]$$

where:

w_i = weight

p = power parameter

n = number of rainfall stations

h_i = distance between the rainfall station to the center of subbasin

h_i is determined from distance equation;

$$h_i = \sqrt{(x - x_i)^2 + (y - y_i)^2} \qquad [9]$$

where:

(x, y) = coordinates of the center of subbasin

(x_i, y_i) = coordinates of rainfall station

Table 5: Weights of rainfall stations in each subbasin

Station Name	Subbasin1	Subbasin2	Subbasin3	Subbasin4	Subbasin5	Subbasin6
Mt Campana	0.51	0.61	0.65	0.28	0.09	0.03
Boso Boso	0.37	0.18	0.25	0.18	0.13	0.04
Mt Aries	0.09	0.11	0.07	0.18	0.24	0.06
Mt Oro	0.03	0.10	0.03	0.36	0.54	0.87
Total	1.00	1.00	1.00	1.00	1.00	1.00

Calibration of HBV model was done manually using the trial and error method. But before calibration, initialization of the model was done to condition the model. Data used for model initialization was from January 1, 2002 to June 8, 2003. Calibration followed using the data from June 8, 2003 to June 8, 2004. The validation data was from June 8 up to December 31, 2004. Usually, a 10-year daily time series data is used in calibrating and validating HBV model (Lindstrom et al., 1997). This is one of the limitations of this study because there was a limited time series data available in the study area. Table 6 shows a list of sensitive parameters used in HBV calibration.

Table 6: List of parameters used in the HBV calibration

Model Routine	Parameter	Description
Soil Moisture	*FC*	Maximum soil moisture storage
	LP	Limit for potential evaporation
	Beta	Exponent in the equation for discharge from the soil water zone
Response Function	*K4*	Recession coefficient for the lower response box
	Khq	Recession coefficient for the upper response box when the discharge is *Hq*
	Hq	Calculated value (see equation 5)
	Alfa	Used in the equation $Q_0 = K \bullet UZ^{(Alfa+1)}$

4.3. DUFLOW Model

4.3.1. Model Background

DUFLOW Modelling Studio (DMS) is a window-based water quantity and quality computer code. DMS has a user friendly interface making it easy to use, manipulate and understand. The interface has a context sensitive menu and short cut tool bars that can contribute to a quick operation of the system.

The DUFLOW Modelling Studio consists of four main components (Stowa/MX.Systems, 2004b):

- DUFLOW water quality and quantity
- RAM precipitation runoff module
- Tewor
- MODUFLOW

Using the DUFLOW water quantity module, one can perform unsteady flow calculations in an open water course systems. The DUFLOW water quality module is useful when modelling the transport of substance in free flowing water and can also model even in more complicated water quality processes. RAM precipitation runoff module was developed to calculate the contribution of precipitation to the surface flow. This module simulates the surface flow by calculating the losses from precipitation and delays in runoff. Tewor module is useful in calculating the discharge in sewer systems and can also be used in modelling water quality in an urban environment. The MODUFLOW module is a

combination of MODFLOW and DUFLOW. It models the interaction of both surface water and groundwater.

DUFLOW is based on the one dimensional partial differential equation that describes unsteady flow in open channels. The following are the equations used in DUFLOW (Stowa/MX.Systems, 2004a):

The conservation of mass equation;

$$\frac{\partial B}{\partial t} + \frac{\partial Q}{\partial x} = 0 \qquad [10]$$

The momentum equation;

$$\frac{\partial Q}{\partial t} + gA\frac{\partial H}{\partial x} + \frac{\partial(\alpha Q v)}{\partial x} + \frac{g|Q|Q}{C^2 AR} = a\gamma w^2 \cos(\Phi - \phi) \qquad [11]$$

while the relation;

$$Q = v \cdot A \qquad [12]$$

holds and where;

t	= time	[s]
x	= distance as measured along the channel axis	[m]
$H(x,t)$	= water level with respect to reference level	[m]
$v(x,t)$	= mean velocity (average over the cross sectional area)	[m/s]
$Q(x,t)$	= discharge at location x and at time t	[m^3/s]
$R(x,H)$	= hydraulic radius of cross section	[m]
a (x,H)	= cross sectional flow width	[m]
$A(x,H)$	= cross sectional flow area	[m^2]
$b(x,h)$	= cross sectional storage width	[m]
$B(x,H)$	= cross sectional storage area	[m^2]
g	= gravitational acceleration	[m^2/s]
$C(x.H)$	= coefficient of De Chezy	[$m^{1/2}$/s]
$w(t)$	= wind velocity	[m/s]
$\Phi(t)$	= wind direction	[degrees]
$\phi(x)$	= direction of channel axis, measured clockwise from north	[degrees]
$\gamma(x)$	= wind conversion coefficient	[-]
α	= correction factor for non-uniformity of the velocity distribution in the advection term, defined as:	[m^2]

$$\alpha = \frac{A}{Q^2}\int v(y,z)^2\, dydz \qquad [13]$$

where the integral is taken over the cross section A.

4.3.2. Initial and Boundary Conditions

Boundary conditions are important inputs in a hydraulic model. It introduces the influence of external system to the model domain through a connecting node. In DUFLOW, physical boundaries may be specified as a constant value or a time series data of water level, river discharge or a relation between the two. Flow going inside the model domain is assigned a positive value and outgoing flow a negative.

Initial condition is necessary when starting a numeric model simulation with a distributed physically based model approach (Rientjes, 2007). DUFLOW requires data of water level or discharge for its initial condition. This data may either be historical measurements, obtained from former computations or just a first reasonable guess.

4.3.3. Model Calibration

Model calibration is the process of finding the optimum values of model parameters which will give the least difference between the observed and the simulated values. The main parameter that is fine tuned is the roughness coefficient of the surface. Usually, Strickler-Manning's roughness coefficient (*k*) is the one used in the calculations.

Calibration is commonly done manually by optimizing the parameter values, starting from the given initial values, until the simulated variable fits with the observations. Calibration is being assessed through visual interpretation and some other statistical means. For this research, calibration results were quantified by the Nash-Sutcliffe model efficiency coefficient (equation 7).

4.3.4. Model Setup

This research used the DUFLOW water quantity module and the RAM precipitation runoff module. DUFLOW quantity module was used to model the flow along the upper Marikina River from Montalban water level station to Mangahan water level station. Data from Montalban station was used as the upstream boundary condition and the data from Mangahan station was used as the downstream boundary condition. The distance between these two stations is about 20.10 kilometers and twelve river cross sections were used. The river cross section profiles for the whole stretch of upper Marikina River are almost the same.

The intermediate area between Montalban station and Sto Nino station was handled by RAM precipitation runoff module. This module was used to compute for the lateral inflow from the intermediate area that drains to upper Marikina River. The intermediate area was assumed to be 100 percent unpaved and was divided into four areas. But since there was a water level gauging station (Nangka station) in one of the divided area, it was excluded from RAM calculations. However, flow from this area, represented by its station was also used as one of the lateral inflows to upper Marikina River.

The three remaining areas (shown as Area1, Area2 and Area3 in Figure 1) used the RAM precipitation runoff module in simulating their respective discharges. Each of the area used a separate rainfall data set based on weights taken from inverse distance method. Calculated weights of rainfall stations are shown in Table 7. Evapotranspiration was computed using Makkink method. Makkink method was originally developed for humid conditions in the Netherlands (Kassam et al., 2001) and might not be applicable to the study area. It is therefore recommended to use other methods that will fit the conditions of the study area in future studies. Other parameter values that were used were based on literature. Table 8 shows the list of parameters used in RAM module and its descriptions. No calibration was done for RAM module because there was no actual data to compare it with. DUFLOW model network is presented in Figure 17.

Table 7: Weights of rainfall stations in each area used in RAM module

Rainfall Station	**Area1 (A=28.21 km^2)**	**Area2 (A=40.12 km^2)**	**Area3 (A=19.05 km^2)**
Nangka	0.16	0.54	0.92
Mt Oro	0.17	0.13	0.02
Mt Campana	0.05	0.03	0.01
Mt Aries	0.50	0.25	0.04
Boso Boso	0.12	0.05	0.01
Total	1.00	1.00	1.00

Table 8: Parameters used in unpaved surface in RAM module

Parameter	**Properties**
I_{max}	Infiltration capacity [mm/hr]
f	Crop factor Makkink [-]
F0	Moisture storage at pF=0 [mm]
F2	Moisture storage at pF=2 [mm]
F4.2	Moisture storage at pF=4.2 [mm]
Phi0	Initial moisture storage [mm]
LBv0	Initial depth of the unsaturated zone [mm]
n	Pore content [-]
BL_{min}	Storage value in linear reservoir at which capillary rise is activated [mm]
$P_{percmax}$	Percolation to unsaturated zone between pF=0 and pF=2 (maximum) [mm/hr]
C_{max}	Maximum capillary rise [mm/hr]
$K_{surface}$	Time constant reservoir unpaved surface [hr]
K_{quick}	Time constant fast groundwater discharge [hr]
K_{slow}	Time constant slow groundwater discharge [hr]
B_{slow}	Distribution formula for fast and slow groundwater discharge [-]

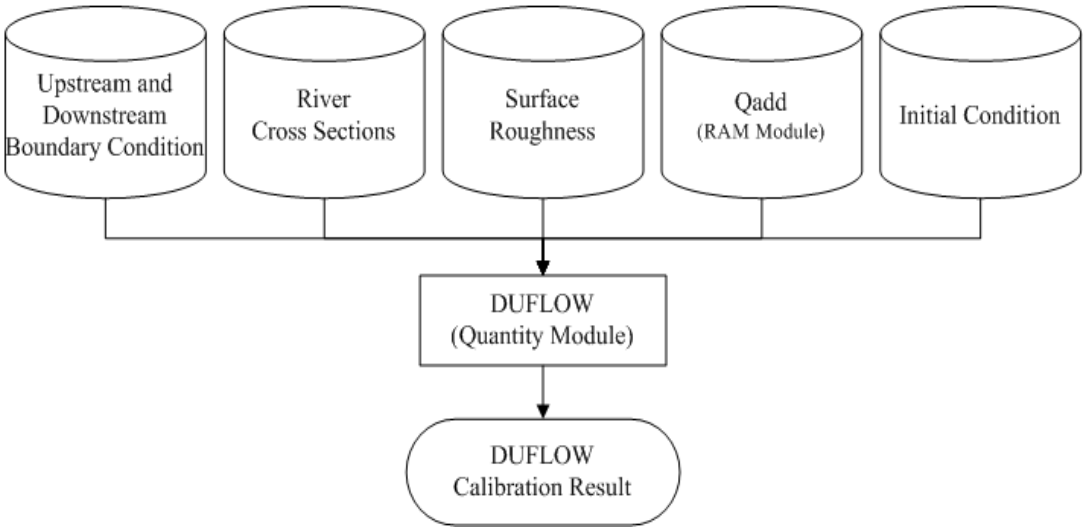

Figure 16: Schematization of model input/output in the DUFLOW water quantity module

Calibration for DUFLOW water quantity module was done at Sto Nino water level station. This station is located downstream of Montalban station and upstream of Mangahan station as shown in Figure 17. Using the optimized parameter set derived during calibration, river flow was again simulated, this time using the simulated hydrograph of HBV model as the upstream boundary condition. The downstream boundary condition remains the same. The resulting hydrographs using different upstream boundary conditions were compared and discussed in section 5.2.2.

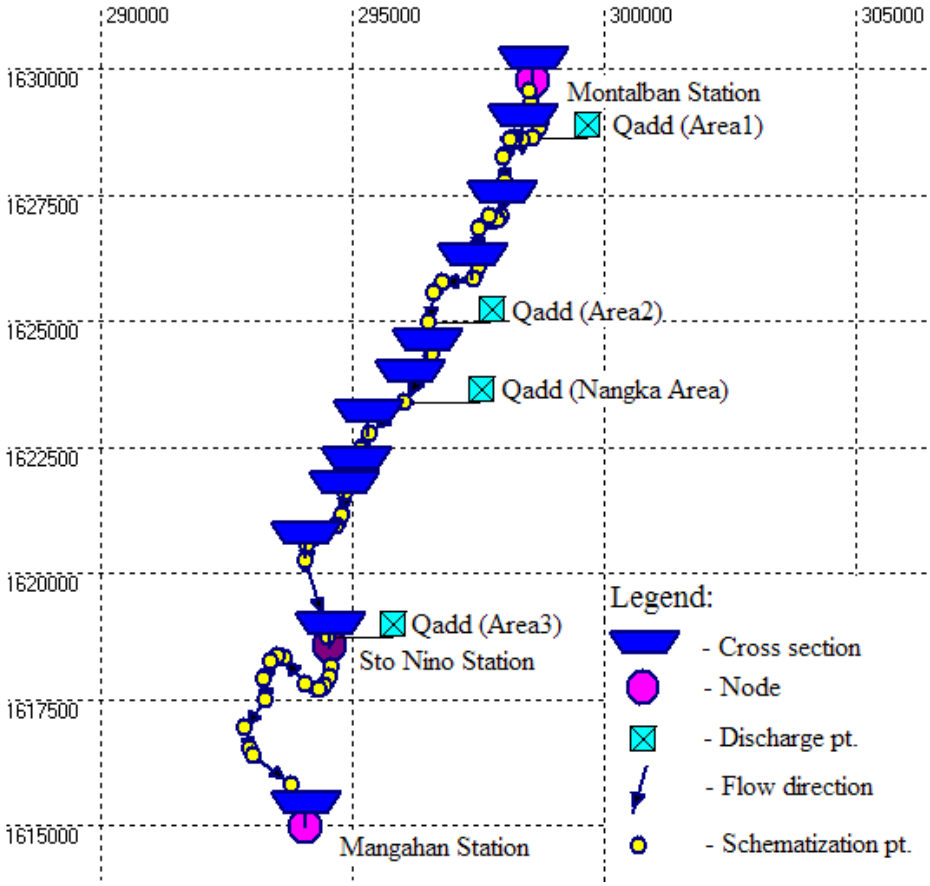

Figure 17: DUFLOW model network

4.4. Data Availability and Preparation

4.4.1. SRTM Elevation Data

Digital Elevation Model (DEM) is a digital representation of a portion of the earth's surface. Digital elevation data are stored in either of the following formats: as point elevation data on either a regular grid or triangular network, or as vector contours stored in a digital line graph. Either of these formats offers advantages for certain applications, but generally, the grid format is the one used most often (Zhang et al., 1994).

The topology which is of great influence in hydrological processes in a catchment can be extracted from a digital elevation model. Many hydrologic models rely on spatially distributed characterization of catchment's slope, river length, flow and direction, and drainage area which can be generated through DEM processing.

The digital elevation model used for this study was extracted from a near-global dataset from Shuttle Radar Topographic Mission (SRTM). It is a free data set and can be downloaded from http:www2.jpl.nasa.gov/srtm/. SRTM elevation data was a product of a joint effort of the National Aeronautics and Space Administration (NASA) and the National Geospatial-Intelligence Agency (NGA) and the involvement of the German and Italian Space Agencies. These agencies were the one responsible in generating the near global digital elevation model of the earth using radar interferometry (NASA, 2005). SRTM data was taken on February 2000 during an 11-day mission which covered areas smaller than 60 degrees latitude.

The digital elevation data from SRTM are distributed in two levels; SRTM1 with data sampled at one arc-second intervals in latitude and longitude and the SRTM3 which was sampled using three arc-seconds. Three by three one arc-second samples were averaged to generate the SRTM3 data. SRTM3 with a resolution of 90 m was used for this study. SRTM1 samples with higher resolution of 30 m are only available for the United States of America and its territories and possessions. The horizontal datum for the SRTM data set is the World Geodetic System 1984 (WGS84) and vertical datum is Mean Sea Level (MSL) as determined by Earth Gravitational Model (EGM) 1996.

Table 9 indicates the SRTM data equivalent in Digital Terrain Elevation Data (DTED) which is in a form of uniform matrix of terrain elevation values. DTED can provide basic information to applications that require terrain elevation, slope and surface roughness. However, DTED is only used for military applications. Digital Terrain Elevation Data Level 0 (DTED0) has an elevation posting of 30 arc-second (nominally one kilometer). DTED1 has a basic medium resolution sampled in every three arc-seconds, approximately 100 meters. The information content is approximately equivalent to the contour information represented in a 1:250,000 scale map. DTED2 is sampled in every one arc-second, approximately 30 meters. The information content is equivalent to the contour information represented on a 1:50,000 scale map (Pike, 2000).

Table 9: SRTM data naming conventions

Posting (Sample Spacing)	SRTM Name	DTED Equivalent
1 arc-second	SRTM1	DTED2 (Indicating 'level 2')
3 arc-second	SRTM3	DTED1 (Indicating 'level 1')
30 arc-second	SRTM30	DTED0 (Indicating 'level 0')

Source: NASA (2005)

The accuracy of SRTM elevation data was tested by Rodriguez et al. (2005) using Kinematic Global Positioning System (KGPS) transects. The KGPS data were collected using vehicles carrying Global Positioning System (GPS) receivers along roads throughout the mapped areas. KGPS method produced data representing a non-uniform sampling of latitude, longitude and height along the surface feature. A typical KGPS transect span runs a significant part of a continent thereby allowing for the characterization of errors at all length scales. The total number of samples collected reaches to nearly 9.4 million and covers six continents. Table 11 shows the summary of SRTM data performance compared to the KGPS transects. It is clear from Table 11 that SRTM elevation data met and exceeded its performance requirements which are shown in Table 10.

Table 10: Performance requirements for the SRTM data products

Error	SRTM Performance Requirement (m)
Linear vertical absolute height error	16
Linear vertical relative height error	10
Circular absolute geolocation error	20
Circular relative geolocation error	15

Source: Rodriguez et al. (2005)

Table 11: Summary of SRTM data performance

Error	Africa (m)	Australia (m)	Eurasia (m)	Islands (m)	N America (m)	S America (m)
Absolute Geolocation Error	11.9	7.2	8.8	9.0	12.6	9.0
Absolute Height Error	5.6	6.0	6.2	8.0	9.0	6.2
Relative Height Error	9.8	4.7	8.7	6.2	7.0	5.5

Source: Rodriguez et al. (2005)

Gorokhovich et al. (2006) conducted another research on the accuracy of SRTM-based elevation data. Their research covers the area of Catskill Mountains in New York and in Phuket in Thailand. The result of their research proved that the actual accuracy of SRTM-based elevation data was significantly better than the performance requirement for the SRTM product. For the Phuket area, the absolute average vertical error was 7.58 +/- 0.60 m and for the Catskill Mountains, the error was about 4.07 +/- 0.47 m. The result of their research confirmed the work done by Rodriguez et al. (2005) that

the actual accuracy of SRTM elevation data is significantly better than the standard performance requirement indicated in Table 10.

This study will make use of the extracted parameters from the digital elevation model. However, accuracy assessment of the digital elevation model and extracted parameters will not form part of this research.

4.4.2. Catchment Extraction from DEM

Catchment extraction from the digital elevation model was done using the Integrated Land and Water Information System (ILWIS version 3.3). The study area, the Pasig-Marikina River Basin, was extracted from the downloaded SRTM elevation data using the DEM hydro-processing menu in ILWIS. The DEM hydro-processing module has a well structured sequential menu for catchment extraction from DEM. The extracted catchment has a total area of 377.82 square kilometers. The highest point is 1122 m and the lowest point is 28 m with the longest flow path of 42.85 km. The catchment area was divided into 6 subbasins and the subbasins were again divided into different zones. Each zone was further divided into different vertical layers of 100 m interval. In HBV model, corrections for rainfall and temperature is done using 100 m elevation interval.

4.4.3. Rainfall Data

Rainfall data is one of the most important inputs in hydrological modelling because it is the driving force in a catchment runoff. In rainfall runoff modelling, accurate knowledge of rainfall distribution is a prerequisite in accurately estimating discharge. This is because rainfall distribution over a catchment is a vital factor in determining surface runoff processes (Syed et al., 2003). However, it is difficult to accurately represent rainfall in hydrological models because its distribution varies over space and time. Beven (2000) said that there is no any model that can predict accurate hydrograph if the input rainfall does not represent the real distribution over the catchment.

Rainfall data used for this study was obtained from EFCOS. EFCOS is the agency taking charge in the operation and maintenance of Pasig-Marikina River Basin. Hourly rainfall data was collected during the fieldwork for four stations for the year 2002, 2003 and 2004. Nangka rainfall data was also collected but only for the year 2003 and 2004 because this is a new station. Table 12 shows the rainfall stations and their corresponding elevations extracted from DEM. The rainfall data was found to be homogeneous when tested as shown in Figure 18. The homogeneity test was used to check for missing data in a time series. If there are missing data, the solid line in Figure 18 will fell below the broken line. Nangka rainfall data was not used in HBV model setup because of the reason cited above and was not included in the homogeneity test.

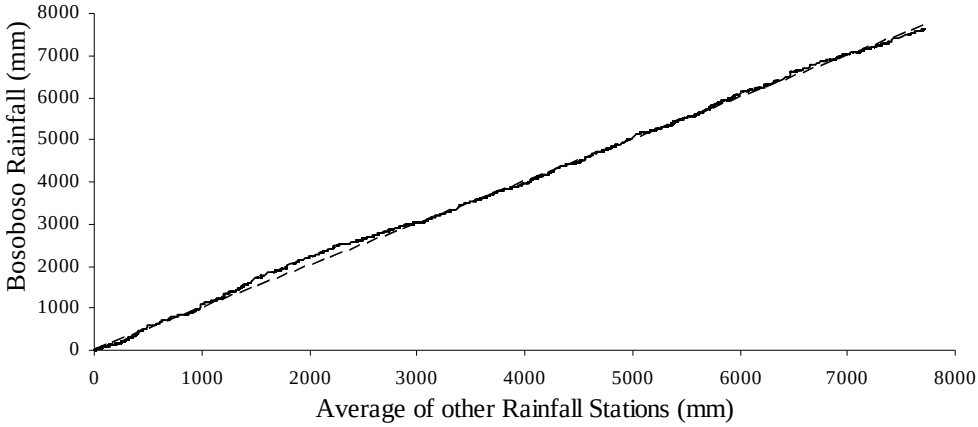

Figure 18: Rainfall homogeneity test

Table 12: Rainfall stations, location coordinates and elevations

Rainfall Station	Latitude	Longitude	Elevation (m amsl)
Mt Campana	1622201.3	315962.9	519
Boso Boso	1619159.8	308613.9	374
Mt Aries	1621750.9	302816.8	392
Mt Oro	1632825.1	301722.3	55
Nangka	1623243.4	296257.6	20

The distribution of rain gauges over the catchment is not ideal as shown in Figure 1. Three rainfall stations are located within Pasig-Marikina River Basin while the other two are located outside the catchment area. Mountainous areas were not properly represented because there were no rain gauges located in those areas. Mt Campana which is the most elevated rainfall station has only an elevation of 519 m. The highest point in the catchment is around 1122 m.

The rainfall distribution within the catchment is highly variable over space and in time. This could be the result of a very complex rainfall pattern over the area. The study area is situated between two large water bodies, the South China Sea in the west and the Pacific Ocean in the east, and is frequented by many types of weather systems. Some of the rain bearing weather systems that affect the area includes; tropical cyclones, southwest monsoons, intertropical convergence zones (ITCZ) and some localized convective activities.

4.4.4. Water Level Data

Water level data used for this study was provided by EFCOS. Hourly water level data for Montalban, Sto Nino, Mangahan and Nangka stations for the year 2002, 2003 and 2004 were collected during the field campaign. Aside from the water level data, rating curve for Montalban and Sto. Nino stations were collected.

For this research, Montalban water level data was used to calibrate the HBV model. DUFLOW model used both Montalban and Mangahan water level data as upstream and downstream boundary conditions, respectively and calibration was done using the Sto Nino water level data.

4.4.5. Land Cover Data

The land cover map for the study area was provided by the National Mapping and Resource Information Authority (NAMRIA). The land cover map was reclassified according to the type of zones applied in HBV model. The types of zones used in the HBV model were; forest, field, glacier and lakes. For the study area, only forest and field are the applicable zones. Lakes and glaciers zones were not used for this research.

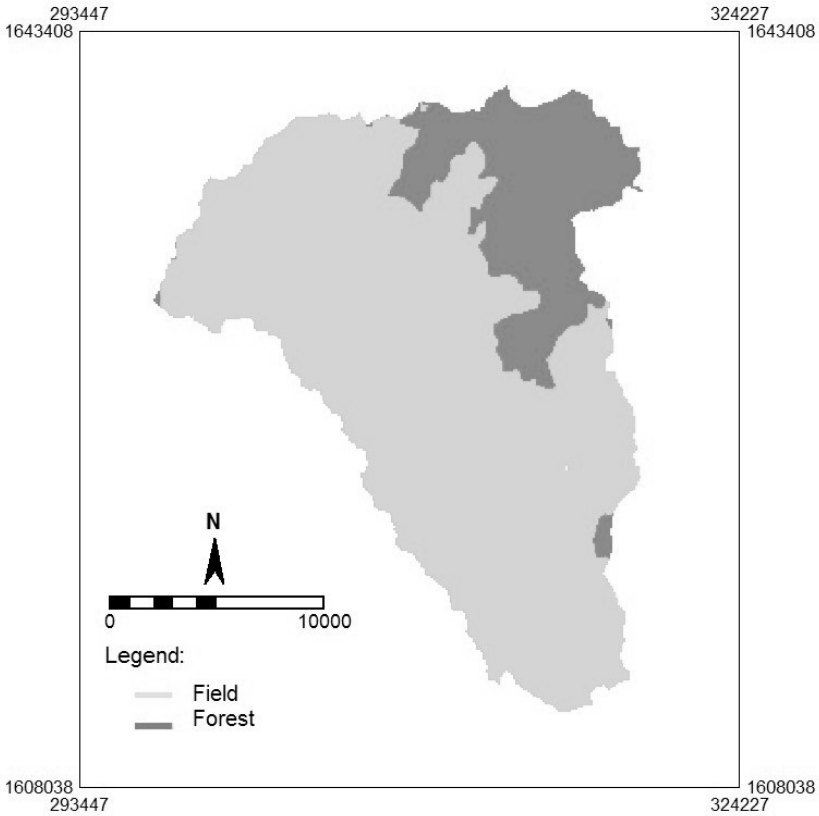

Figure 19: Reclassified land cover map

4.4.6. River Cross Sections

River cross sections for the Marikina River were obtained from different sources. River cross sections in Montalban, Sto Nino and Nangka water level gauging stations were provided by EFCOS. Cross sections from Sto Nino water level gauging station down to Mangahan station were provided by Woodfields Consultants, Inc. (WCI) through the Department of Public Works and Highways (DPWH). Data sets collected from WCI are river cross sections with an interval of 50 meters along the length of the river.

River cross sectioning activities were undertaken during the fieldwork in sections between Montalban and Sto Nino water level gauging stations. A total of nine cross sections were surveyed during the field campaign. Figure 20 shows some pictures taken during river cross sectioning activity. In most cases, wading across the river was required because boats were not available. The instrument used during the survey was a total station provided by the Flood Forecasting Branch of PAGASA.

Figure 20: Survey group conducting river cross sectioning activities

5. Results and Discussions

5.1. HBV Model

5.1.1. Model Performance

The HBV model was setup as described in section 4.2.5. The rainfall data was divided into three parts. The first part was used in initializing the model. The second part was used for calibration and the third part was utilized in validating the calibrated model. The purpose of initialization is to let the model adopt the hydrological mode of the modelled environment. Calibration was done at the outlet of the catchment (Montalban station) and was done manually by trial and error method. The best model parameter combination which gave the optimum result is given in Table 13. The resulting Nash-Sutcliffe efficiency coefficients (R^2) were 0.79 for calibration and 0.76 for validation. The accumulated difference for calibration and validation were -291.60 and +362.78 millimeters, respectively.

Table 13: Best parameter set used in HBV model

Model Routine	Parameter	Calibrated value
Soil Moisture	*FC*	300
	LP	0.98
	Beta	2
Response Function	*K4*	0.1
	Khq	0.2
	Hq	18.7
	Alfa	1.1

Figure 21 shows the discharge hydrograph after calibration. The figure shows that the model was able to accurately simulate the timing of the hydrograph. However, some disagreements between the observed and the simulated hydrograph were seen at some peaks. The most obvious discrepancy between the two data sets was on the peak of September 2, 2003. The simulated peak during that instant was 998.70 m^3/s while the observed was 1,344.10 m^3/s. It has a difference of 345.40 m^3/s which translates to 0.58 meters when the discharge hydrograph was converted to water level hydrograph using the acquired rating curve. The water level hydrograph is shown in Figure 22.

The hydrograph peak that occurred on September 28, 2003 showed that the simulated hydrograph was 806.70 m^3/s while the observed hydrograph was 648.3 m^3/s. The difference translates to 0.34 meters when the discharge hydrograph was converted. But while the hydrograph difference on the 2nd September reveals underestimation on the part of simulated hydrograph, the difference in 28th September shows overestimation. Some other peaks are either overestimated or underestimated but there are also few peaks which were simulated well.

The baseflow difference between the observed and simulated hydrographs as shown in Figure 21 cannot be clearly seen because of the limitation of the vertical scale. However, since discharge is a direct function of water level, Figure 22 must be used in discussing the baseflow. Figure 22 clearly shows that the baseflow is underestimated on majority part of the hydrograph during the calibration period. There was a little portion at the end of this hydrograph which is overestimated and it continues to the early part of the validation period (Figure 24).

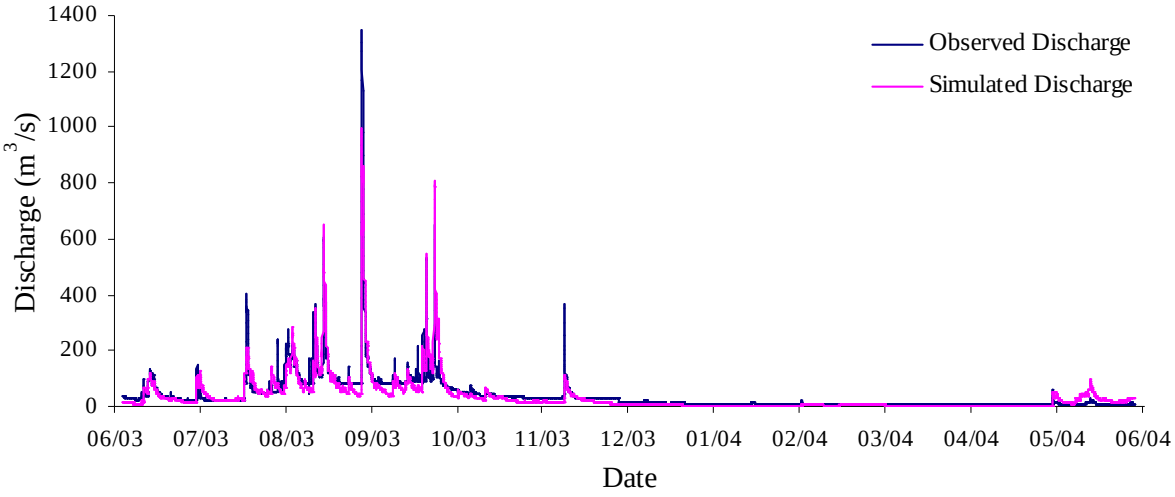

Figure 21: HBV model calibration result shown as discharge hydrograph

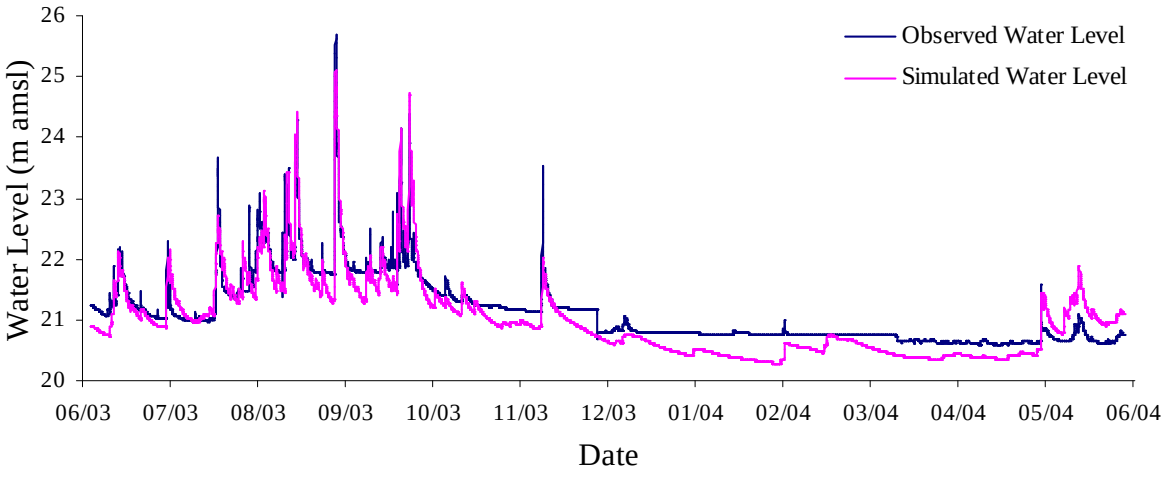

Figure 22: HBV model calibration result shown as water level hydrograph

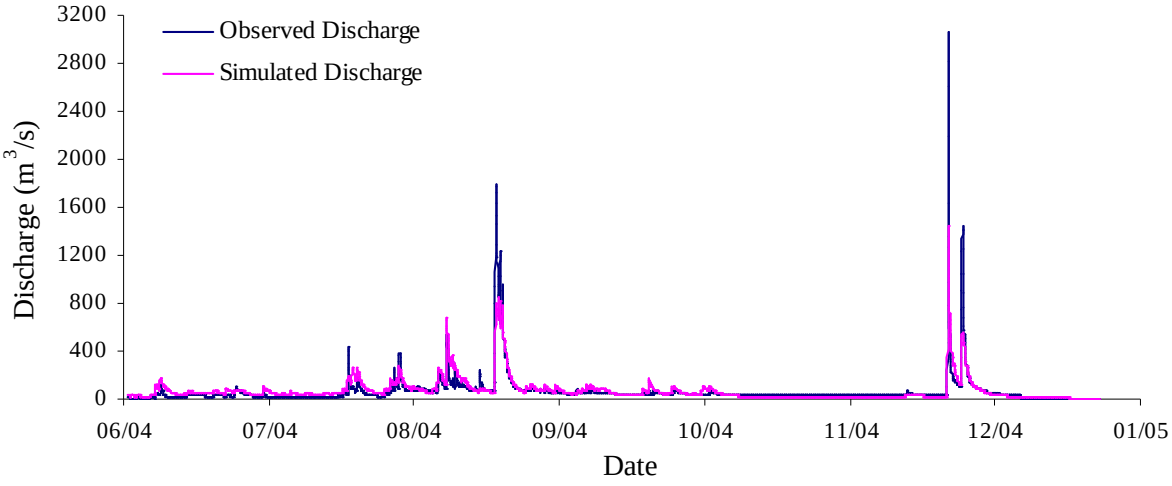

Figure 23: HBV model validation result shown as discharge hydrograph

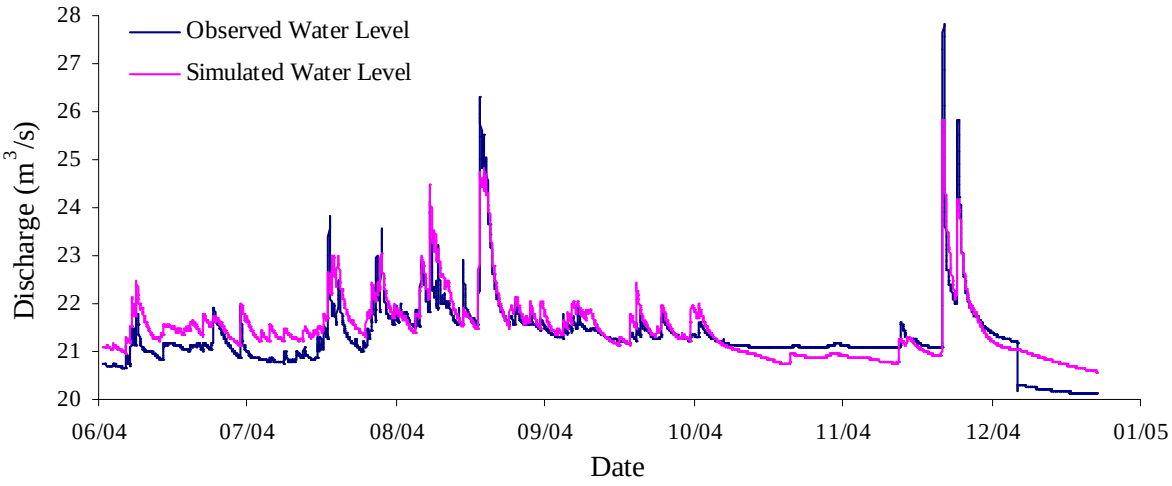

Figure 24: HBV model validation result shown as water level hydrograph

5.1.2. Model Uncertainty

The disagreements between the observed and the simulated hydrographs could be attributed to model uncertainties. Abbott et al. (1996) identified four possible sources of model uncertainties, they are:

1. Random or systematic errors in the input data
2. Random or systematic errors in the recorded data
3. Errors due to non-optimal parameter values
4. Errors due to an incomplete or biased model structure

The first two sources could be attributed to data uncertainty. Input data is used to represent the condition of the model in space and in time. Examples of input data used in HBV are rainfall, temperature and evapotranspiration. Recorded data are used to evaluate the result of the simulation. For this study, only water level can be considered as a recorded data that is shown in Figure 22 and

24. By personal communication, thesis supervisors have indicated that some time series shown some erratic values and that time series must be analysed for consistency. This is particular for baseflow observations and some isolated periods. It was suggested that debris has affected the observations. The third cause could be associated with the calibration process and the last one could be caused by the model's simplification processes. Rainfall is the main driving force in a basin's runoff. For the HBV model, only four rainfall stations were available for the study area. The distribution of these rainfall stations over the study area is not considered ideal for modelling because rainfall stations were mostly located in areas with relatively low elevations. Mt Campana which is the highest elevated rainfall station has its station elevation less than half of the elevation of the highest mountain summit.

Generally, rainfall increases with an increase in elevation. Therefore, proper representation of rainfall with respect to space (elevation) is a must to have a better simulation result. By Figures 21 and 23 and Figures 22 and 24, it could be seen that almost always the peak of the hydrograph is underestimated. This could be the result of not properly representing rainfall in areas higher than Mt Campana station. It is however recognized that installing rainfall stations on those peaks are expensive and difficult to maintain.

In modelling, large number of required parameters to calibrate a model is often the main cause of uncertainties due to non-optimal parameter values. For this study, calibration of HBV model was done manually by trial and error method. Since there are quite a number of parameters to be calibrated, it is very difficult to find the optimum parameter combination because the state of equifinality may occur. Equifinality is the state wherein different parameter sets produced similar results (Beven et al., 2001). This problem is a major issue in hydrological modelling and is most common to hydrological models which use a lot of parameters. However, equifinality may also occur even in parsimonious models.

Errors due to an incomplete or biased model structure could be associated with the model simplification of reality. The real world is too complex to model and representing every aspect of it is impossible. Models are simplified versions of the processes in the real world in mathematical form. Due to simplification, some aspects of the real world are sometimes lumped and/or neglected. This simplification introduces errors in representing the physical characteristics of the real world. In HBV model, simplifications were done in almost all input data from rainfall to land cover. Rainfall data in each subbasin was computed using inverse distance method considering only the center of the subbasin. The center of the subbasin could have different weights from the points away from it. Land cover was also reclassified into only two land covers despite the fact that in reality it has more classes. However, having a model, distributed or lumped, is better than doing nothing.

5.1.3. Sensitivity Analysis

Sensitivity analysis is usually performed during calibration of models to determine which parameters are sensitive and is likely to have a dominant effect on the result of the simulation (Haile, 2005). This is done by changing the values of parameters one at a time. HBV model has a considerable number of parameters for calibration but the most dominant ones were selected by sensitivity analysis. The

parameter values were plotted against the Nash-Sutcliffe efficiency coefficient (R^2) values to show the change in R^2 with the change in the parameter values.

Parameter *Alfa* is one of the most sensitive parameters in HBV. It was used in simulating for the outflow from the upper reservoir as shown in equation [3]. A low value of *Alfa* resulted to less runoff from the upper reservoir (*UZ*) thereby decreasing the dynamic response of the model. This resulted to underestimation of the peaks but the baseflow has a better fit. A high value of *Alfa* makes the model more dynamic draining almost all water from the upper reservoir to the river making the hydrograph peaks high but the groundwater was also depleted. This resulted to a big difference in baseflow during summer. The highest value of *Alfa* best described the modelled system yielding the highest R^2.

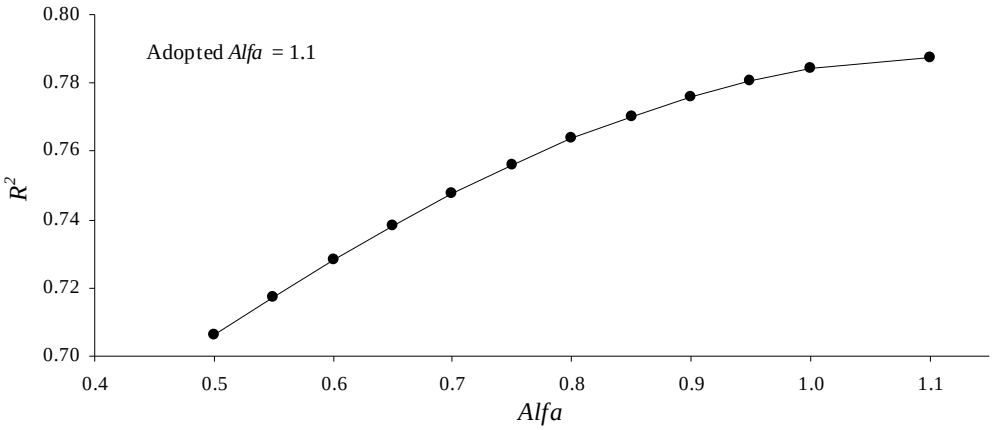

Figure 25: Relation between *Alfa* and Nash-Sutcliffe efficiency coefficients (R^2)

Field capacity (*FC*) is another sensitive parameter in the HBV model. The resulting R^2 on different values of *FC* are shown in Figure 26. When *FC* was set to low values, the soil matrix tends to hold less water and increases immediate flow to response function fitting the high peaks properly. However, just like the effect of high *Alfa* value, the model gives less water during summer. Moreover, even if the minimum value of *FC* was used, the peak on September 2, 2003 was still underestimated. When *FC* was set to its maximum value, almost all rainfall was stored in the soil matrix releasing less water for immediate runoff making a big difference between the observed and the simulated peaks. However, high value of *FC* resulted to a good fit in the baseflow especially during summer.

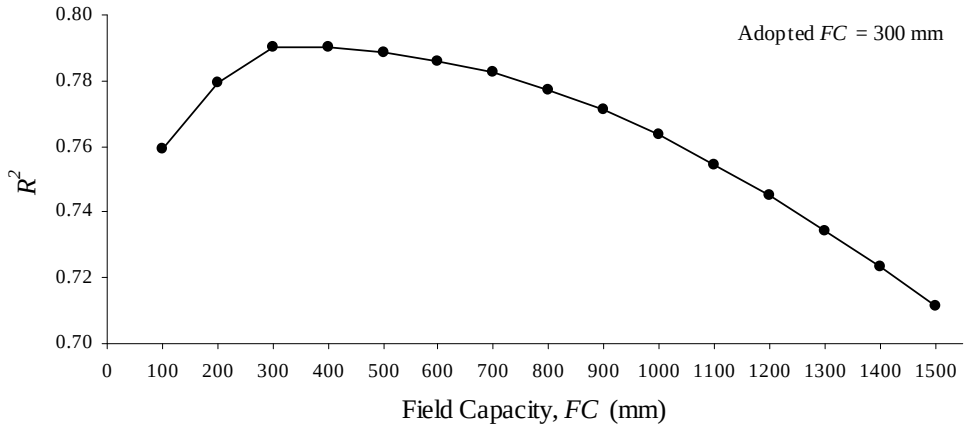

Figure 26: Relation between *FC* and Nash-Sutcliffe efficiency coefficients (R^2)

The most sensitive HBV model parameter is the *Khq*. This parameter controls the recession of the upper response box. Using high values of *Khq* resulted to good simulation in hydrograph peaks. When the lowest value was used, the whole hydrograph was converted to just one wave as shown in Figure 28.

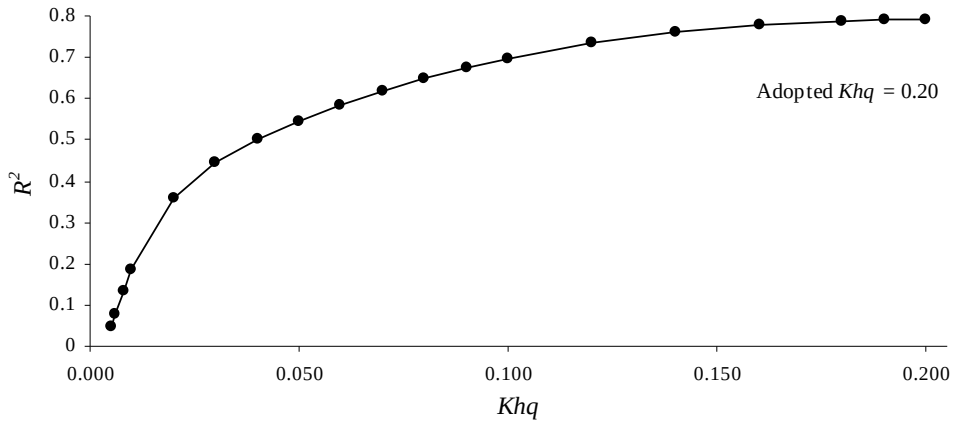

Figure 27: Relation between *Khq* and Nash-Sutcliffe efficiency coefficients (R^2)

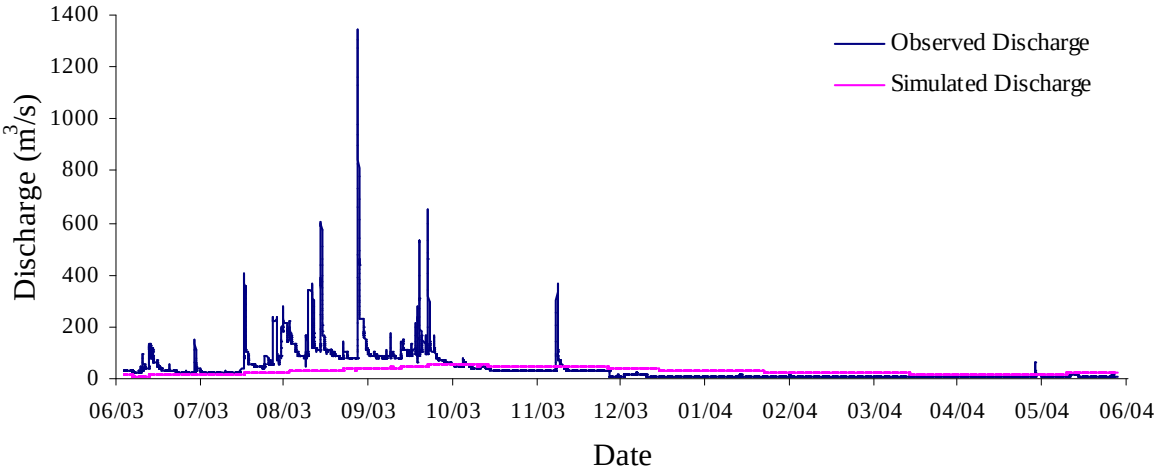

Figure 28: Simulated hydrograph using the minimum value of *Khq*

5.2. DUFLOW Model

5.2.1. RAM Precipitation Runoff Module

The setup of the DUFLOW model was described in section 4.3.4. The intermediate area between Montalban station and Sto Nino station was handled by RAM precipitation runoff module. The three areas mentioned in section 4.3.4 were used to simulate lateral inflows using the parameter values shown in Table 14. Descriptions of these parameters are found in Table 8. Parameter values used for this simulation were taken from literature because these were not available from the field. Also, calibration was not done for this module because discharge data was not available. Figure 29 shows the result of the simulation. Results revealed that the area is directly proportional to the discharge. Area2 which has the biggest area also obtained the highest flow and area3 which is the smallest has

the smallest discharge. The resulting discharges, including the discharge from Nangka area were added to the flow in upper Marikina River as lateral inflows. These inflows were represented as new discharge point (Qadds) in Figure 17.

Table 14: Parameter values used in unpaved surface in RAM Module

Parameter	Value	Parameter	Value
I_{max}	1.30	BL_{min}	250.00
f	1.00	$P_{percmax}$	0.25
$F0$	336.00	C_{max}	0.25
$F2$	282.75	$K_{surface}$	1.00
$F4.2$	107.25	K_{quick}	2.00
$Phi0$	282.75	K_{slow}	4.00
$LBv0$	100.00	B_{slow}	0.50
n	0.50		

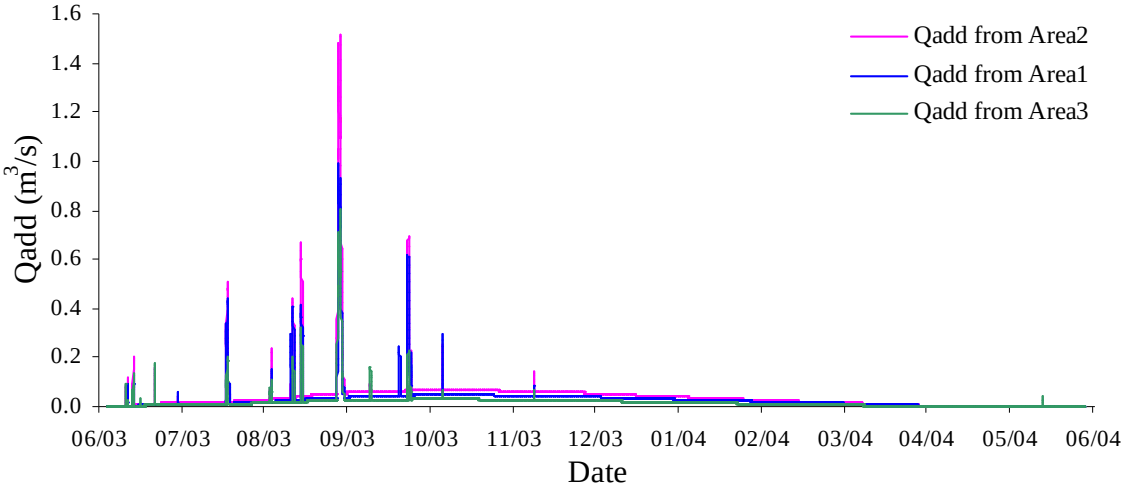

Figure 29: Lateral inflows from intermediate areas computed from RAM module

5.2.2. DUFLOW Water Quantity Module

Simulation result using Montalban Water Level Data

The DUFLOW water quantity module was used to simulate the river flow from Montalban station to Mangahan station. Montalban station served as the upstream boundary of the modelled area and the Mangahan station was the downstream boundary. The calibration of the DUFLOW model was done at Sto Nino station. Lateral inflows from intermediate areas were entered into the main river using the Qadds function of the DUFLOW. Calibration was done manually by trial and error method using different values of Strickler-Manning's coefficient (k). The parameter optimization was focused more on the hydrograph peaks rather than the baseflow. This is because this study was designed to be used for the operation of Rosario Weir and NHCS for flood control and early warning operations.

The calibrated value of *k* was 23.81 which is slightly lower than the normal *k* value for a river that best described the modelled river. The upper Marikina River is a natural channel which can be described as a "winding river, clean with some pools and shoals". According to Hoggan (1989), a river that has the above descriptions has a *k* value range of 22.22 to 30.30 with a normal value of 25.0.

Figure 30 shows that the timing of the simulated hydrograph fits well with the observed water level. The peak of September 2, 2003 flood was well simulated with a value of 16.35 m compared to the observed water level of 16.31 m. However, there are small disagreements in the peaks and the baseflow was overestimated. The average flood lag time from Montalban station to Sto Nino station was 4 hours. The R^2 derived during the calibration process was 0.91.

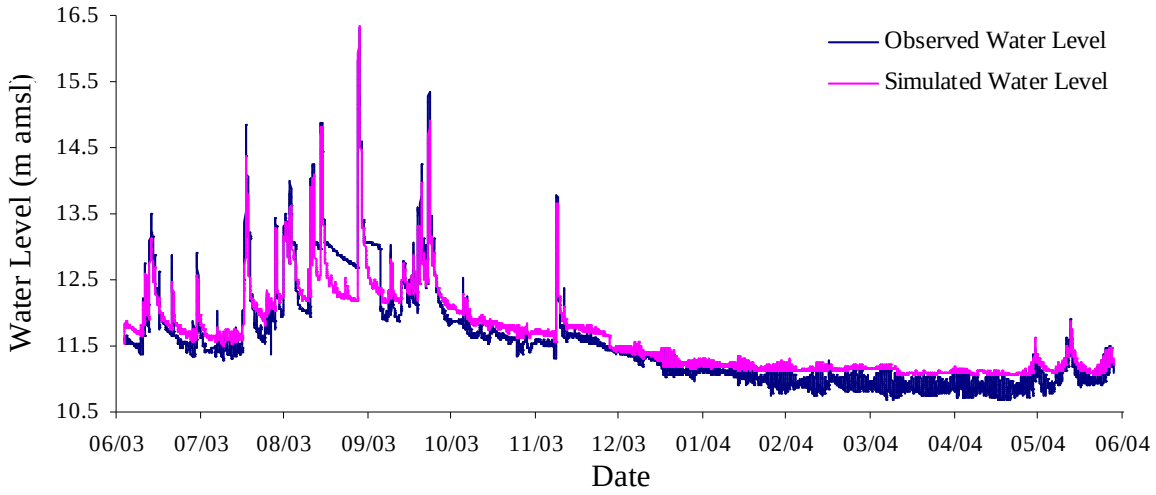

Figure 30: DUFLOW model calibration result using Montalban water level data

Simulation result using HBV Simulated Hydrograph

The optimum set of parameters derived during calibration was used to run the model, this time using the hydrograph from HBV simulation as the upstream boundary condition. This resulted to a Nash-Sutcliffe efficiency coefficient (R^2) of 0.90. Figure 31 shows the result of the simulation compared with the observed hydrograph. It could be seen that timing and the baseflow of the simulated hydrograph fits well with the observation. However, some discrepancies can be observed during peak flows. The hydrograph showed that peak flows were almost always underestimated.

The September 2, 2003 peak which was simulated well during calibration was slightly underestimated. This was caused by the inability of the HBV model to simulate this peak during its calibration. The discrepancy between the observed and the simulated hydrograph during the HBV's simulation has propagated downstream and caused this underestimation. However, this discrepancy was attenuated when the flood propagated down the river channel. During this flood event, the difference between observed water level and the HBV model simulation result at Montalban Station was 0.58 m. This difference was reduced to 0.17 m at Sto Nino station after DUFLOW simulation.

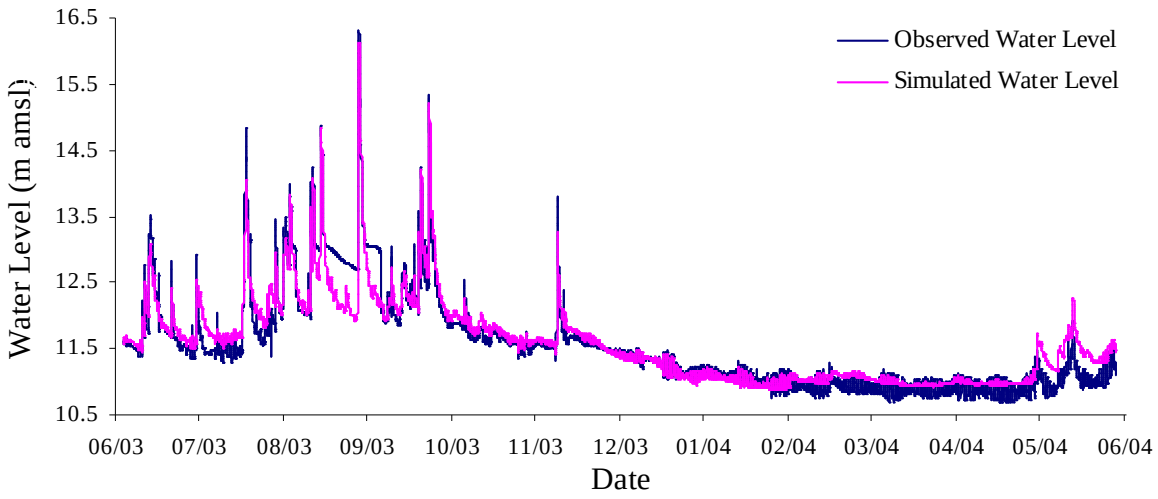

Figure 31: DUFLOW model result using the simulated hydrograph of HBV

Comparison of Model Results

Figure 32 shows the results of DUFLOW simulations using both the Montalban observed data and the simulated hydrograph of HBV as upstream boundary conditions. The simulated hydrograph using Montalban observed data fits with the peaks well although some small disagreements can still be seen. The peak of September 2, 2003 flood was simulated well giving 16.35 m versus the observed data of 16.31 m. However, the model overestimated the entire low flow. Using the HBV simulated hydrograph gave a good fit during high and low flows. The difference of 0.17 m during the peak of September 2, 2003 could be attributed to the inherited underestimation in upstream boundary condition as explained in section 5.2.3.

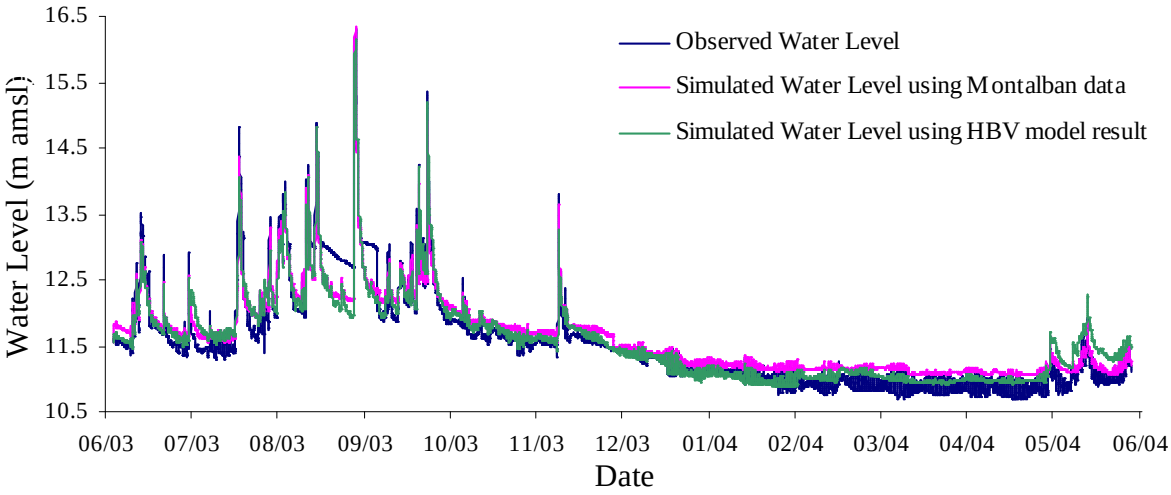

Figure 32: Comparison of the DUFLOW model results

5.2.3. Model Uncertainty

Section 5.1.2 lists the possible sources of model uncertainties according to Abbott et al. (1996). As discussed in section 5.1.2, representation of rainfall over the catchment is an important factor in modelling. In RAM, five rainfall stations were used in estimating the spatial distribution of rainfall over the area. But even if there were five rainfall stations used, it might still not be able to represent the real rainfall distribution because of its complexity. Soil characteristics which were basis on some parameters were just taken from the literature. Also, for this model, soil characteristics in the unpaved surface were assumed to be homogeneous thereby neglecting the heterogeneity of the catchment.

The DUFLOW quantity module uses recorded water level data as its upstream and downstream boundary conditions. It also uses a recorded water level to compare with the simulated results during calibration. Random or systematic error in the recorded data is one of the possible sources of model uncertainty according to Abbott et al. (1996). DUFLOW also used the simulated hydrograph from the HBV model which also utilized data with a certain degree of uncertainty. Errors accumulated in the HBV model can propagate to the DUFLOW model and affect the results. Another possible source of error in the DUFLOW model simulation is the surface roughness coefficient. DUFLOW only allows one value of roughness coefficient in every cross section. Usually, roughness values for the lower and the upper portion of the river cross section are different. However, because of this limitation, the roughness value for the whole cross section is assumed to be the same. The DUFLOW model has also a deficiency in handling river cross sections. An irregularly shaped river cross section must first be converted to a more or less regular shape before it can be entered into the model. Doing this might introduce some errors in the modelled system.

5.2.4. Sensitivity Analysis

Sensitivity analyses were executed to determine how the hydrograph was affected with different parameter values chosen. For this research, different values of surface roughness were used to determine sensitivity of the peak of the hydrograph during the September 2, 2003 flood. Figure 31 shows the behaviour of the peak using different values of Strickler-Manning's roughness coefficient (k).

As shown in the Figure 33, when the entered value of k was low, the resulting water level was high and if k value was high, the water level is low. The coefficient k acts as resistance to flow. Whenever k value is low, the flow will encounter more resistance from the surface resulting in a lower flow velocity. And since the discharge is held constant, this will result to filing up of water thereby producing higher water level. The reverse is also true. Whenever coefficient k is high, there will be less resistance from the surface and the flood waters will be immediately flushed out from the section resulting to low water level. These arguments can be best explained by Manning's velocity equation shown as equation [14]. Figure 34 demonstrated the effect of using high and low k values in the hydrograph and it also showed that the effects of different k values were more emphasized during high

flows. As for the time of the peak, it was observed that the hydrograph with higher *k* value peaks earlier compared to the one with lower *k*. For this model, the time to peak difference is one hour.

$$V = k \cdot R^{2/3} S^{1/2} \qquad [14]$$

where;

V = Average velocity of the cross section
k = Strickler-Manning's roughness coefficient
R = Hydraulic radius
S = Hydraulic slope

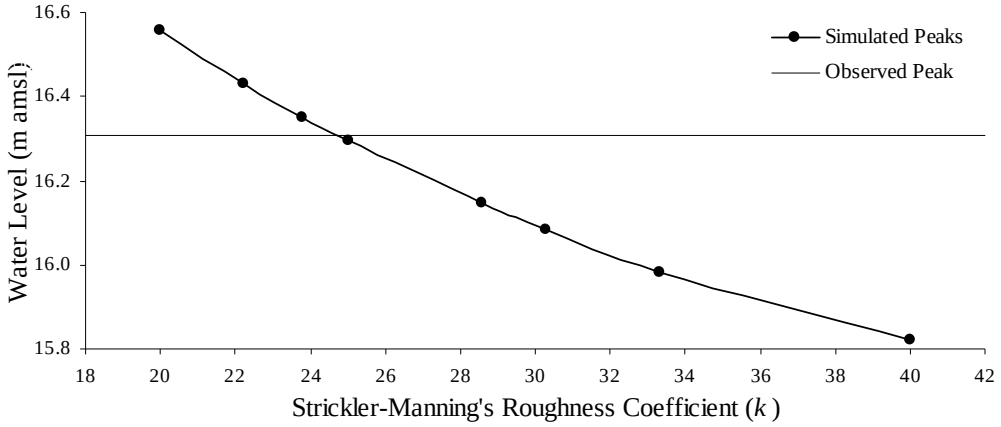

Figure 33: Relation between *k* values and simulated peaks

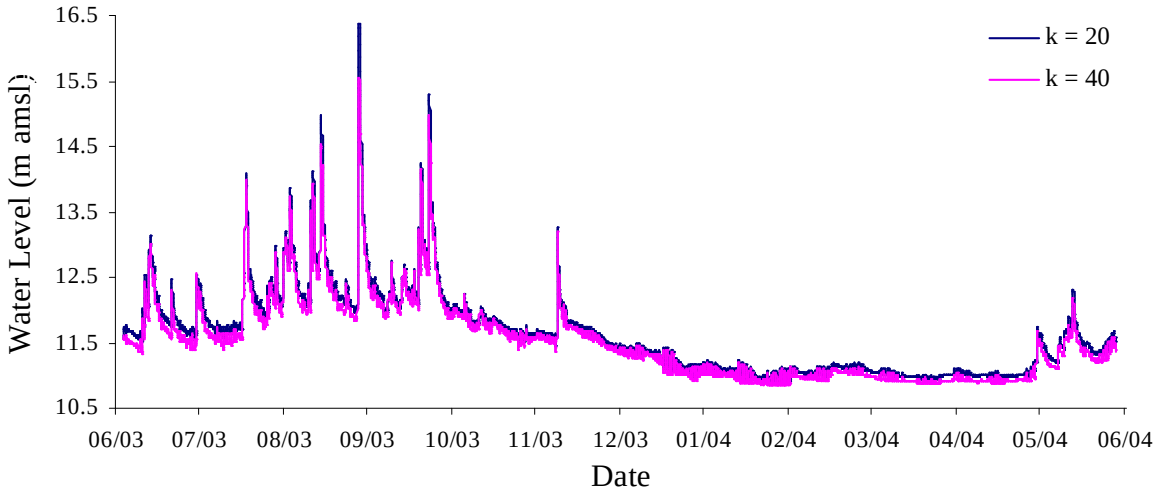

Figure 34: Comparison of hydrographs using high and low *k* values

5.2.5. Model Stability

A numerical model approach such as DUFLOW often introduces inaccuracies to the system and these inaccuracies accumulate as the computation time progresses. When these inaccuracies or errors grow,

it will make the model unstable and the calculation will terminate. In order to have a stable and accurate model, a time step that satisfies the Courant condition (equation 16) has to be adapted (HEC-RAS, 2008).

$$C_r = V_w \frac{\Delta t}{\Delta x} \leq 1.0 \qquad [15]$$

thus, for a stable condition

$$\Delta t \leq \frac{\Delta x}{V_w} \qquad [16]$$

where:

C_r = Courant number
V_w = Flood wave speed
Δt = Computational time step
Δx = Distance between calculation nodes

Flood wave speed is normally greater than the average velocity at a location. One way of approximating the value of flood wave speed is to multiply the average velocity at a location by a factor of 1.5 (HEC-RAS, 2008). The factor of 1.5 is normally used for natural channel. To ensure that the smallest value for the right side of equation [16] was computed, the highest average velocity was chosen from the entire calibration result and was used for the calculation. The calculation yielded 1.72 minutes which is greater than the time step used of 1.0 minute. This means that under Courant condition, the model was accurate and stable. Spitz et al. (1996) said that numeric errors can be minimized if the space and time discretization is sufficiently small and that there is no other technique to address this limitation imposed by finite difference theory.

Stowa/MX.Systems (2004b) recommended some ways of detecting and improving the stability of the DUFLOW model. If the error occurs at the start of the simulation, the most probable cause is the initial condition. This can be addressed by entering a more realistic initial condition data. Doing this will avoid big steps in the network which can cause instability.

Another factor that can be adjusted to have a stable model is the value of *Theta*. *Theta* is a factor that controls numerical damping and its value ranges from 0.5 to 1.0. Highest precision of the results can be obtained when the *Theta* value is at minimum. During this stage, the scheme for solving the shallow water equations is in second order precision in space and time. However, using the minimum value could make the calculation unstable. Using the maximum value makes the model stable but the precision of results is only of the first order in space and time. The adopted value of *Theta* for this study was 0.55.

6. Conclusions and Recommendations

6.1. Conclusions

In this study, two models were applied; the HBV model and the DUFLOW model. The HBV model was applied to simulate the discharge hydrograph of the catchment observed at Montalban station while the DUFLOW model was used to propagate the flood wave from Montalban station to Mangahan station. Both models have been proven to be effective in their respective application field. The HBV model is now in operation in over 40 countries around the world. Although this model was tested with daily data, Kobold et al. (2006) proved that this model can be used for flash floods pre-warning using hourly data. The DUFLOW model is commonly used as a management tool by water authorities. This model is capable of simulating system behaviour due to operations of sluice gates or dams, flood waves, tide waves and operation of irrigation and drainage systems.

The results of the study presented in previous chapters indicated that the calibrated HBV and DUFLOW models can be applied for the flood control and early warning system in the study area. It is further concluded that;

- The HBV semi-distributed model was able to simulate the hydrograph characteristics at Montalban station with Nash-Sutcliffe efficiency coefficient (R^2) of 0.79 for calibration and 0.76 for validation data set. Figures 21 to 24 shows the results of HBV's calibration and validation. The timing of peaks was well simulated although some peaks were underestimated. The underestimations have most likely been caused by improper representation of rainfall over the catchment. As explained in section 4.4.3, rain gauges used for this study were located in the lower part of the catchment. As such, the aerial pattern of rainfall over the catchment was not properly represented resulting to the disagreements in the observed and simulated hydrographs.

- The DUFLOW model was able to satisfactorily simulate the flood propagation along upper Marikina River. Nash-Sutcliffe efficiency coefficient (R^2) of 0.91 was achieved using the observed water level in Montalban station and an R^2 of 0.90 using the simulated hydrograph of HBV model as upstream boundary condition. This model was also able to simulate the effect of backwater flow caused by tide oscillation in Manila Bay. The back flow reached Mangahan station and was indicated as negative discharge in the graph.

- Hydrograph peaks were attenuated as it propagated downstream. Attenuation was caused by flood water storage along the river channel. Storage of flood water along the river channel has a pronounced effect on the hydrograph peak especially if the peak occurs while the water level in the river is still low.

- The HBV model requires data that describes the modelled area. Some of these data such as catchment and sub-catchment areas, elevations, rivers and river flow directions can be extracted from SRTM DEM using a GIS package. This study used ILWIS (version 3.3) in extracting data needed for HBV model simulation. ILWIS has a comprehensive and well structured method of extracting DEM parameters for hydrological models. In ILWIS, this function is called DEM hydro-processing. Under DEM hydro-processing, there is a chronological order of functions used to extract hydrological parameters from DEM. These functions include; DEM visualization, flow determination, flow modification, variable threshold computation, network and catchment extraction, compound parameter extraction and statistical parameter extraction.

- For the HBV model, the computation of lag time was based on the time difference between the peak of the average hourly rainfall and the hydrograph peak at Montalban station. For the DUFLOW model, calculation of lag time was based on the time difference between the hydrograph peaks at Montalban and Sto Nino stations. The computed average flood lag time for the HBV model was 3 hours and 4 hours for the DUFLOW model.

6.2. Recommendations

The performance of the calibrated HBV and DUFLOW models were satisfactory. However, it can still be improved if the following recommendations will be considered;

- To improve the performance of HBV model, it is recommended to use additional rainfall stations around the catchment area so that the aerial distribution of rainfall can be represented well.

- This study uses only three years of hourly rainfall and water level data. It is recommended to use a longer time series data for calibration and validation of the HBV model. This model was developed and tested using ten years of time series data for calibration and another ten years for validation.

- Proper calibration and validation of RAM precipitation runoff module should be done to have a more accurate and reliable simulation in the DUFLOW model. A field survey can help in identifying proper values of parameters to be entered to RAM module.

- Products of rainfall estimation techniques from radars and other satellite sensors will be useful if longer lead time is desired.

References

Abbott, M. B. r., & Refsgaard, J. C. r. (1996). *Distributed hydrological modelling*. Dordrecht etc.: Kluwer Academic.

Andersson, L., Hellstrom, S., Kjellstrom, E., Losjo, K., Rummukainen, M., Samuelsson, P., et al. (2006, December 11, 2006). Climate change impact on water resources in the Pungwe drainage basin. from http://www.pungweriver.net/Download/ENG/Pungwe_CC_%20 Modeling%20Report.pdf.

Aronoff, S. (2005). *Remote Sensing for GIS Managers*. Redlands, California: ESRI.

Bedient, P. B., & Huber, W. C. (1988). *Hydrology and floodplain analysis*. Reading etc.: Addison-Wesley.

Bergstrom, S., & Graham, L. P. (1998). On the scale problem in hydrological modelling. *Journal of Hydrology, 211*, 253-265.

Beven, K. J. (2000). *Rainfall runoff modelling : the primer*. Chichester etc.: Wiley & Sons.

Beven, K. J., & Freer, J. (2001). Equifinality, data assimilation, and uncertainty estimation in mechanistic modelling of complex environmental systems using the GLUE methodology. *Journal of Hydrology, 249*(2001), 11-29.

Burrough, P. A. (1986). *Principles of geographical information systems for land resources assessment*. Oxford: Clarendon Press.

Chow, V. T., Maidment, D. R., & Mays, L. W. (1988). *Applied hydrology*. New York etc.: McGraw-Hill.

CTI Engineering Co. LTD. (1993). Operation and Maintenance Manual for Nationwide Flood Control and Dredging Project, Part B, An Effective Flood Control Operation System Including Telemetering and Flood Warning System in the Pasig-Marikina-Laguna Lake Complex. Manila, Philippines.

de By, R. A., Ellis, M. C., Kainz, W., Knippers, R. A., Kraak, M. J., Krol, B. G. C. M., et al. (1999). *Principles of geographic information systems : ITC core module : version 1 : syllabus*. Enschede: ITC.

Ericta, C. N. (2006, October 5, 2007). Population Projection Statistics. from http://www.census.gov.ph/data/pressrelease/2006/pr0620tx.html.

ESCAP/UN. (1991). *Manual and Guidelines for Comprehensive Flood Loss Prevention and Management*.

ESCAP/UN. (1997). *Guidelines and Manual on Land-use Planning and Practices in Watershed Management and Disaster Reduction*.

FFB/PAGASA (Writer) (2002). Coping with River Flooding [VCD]. In PAGASA (Producer). Philippines.

Google Earth. (2007). Retrieved January 2, 2008, from http://earth.google.com/.

Gorokhovich, Y., & Voustianiouk, A. (2006). Accuracy assessment of the processed SRTM-based elevation data by CGIAR using field data from USA and Thailand and its relation to the terrain characteristics [Electronic Version]. *Remote Sensing and Environment*, 104, 409-415. Retrieved December 28, 2007 from http://www.ciesin.columbia.edu/documents/yuri_ accuracy.pdf.

Haan, C. T. e., Johnson, H. P. e., & Brakensiek, D. L. e. (1982). *Hydrologic modeling of small watersheds*. St. Joseph: American Society of Agricultural Engineers (ASAE).

Haile, A. T. (2005). *Integrating hydrodynamic models and high resolution DEM LIDAR for flood modelling*. ITC, Enschede.

HEC-RAS. (2008). HEC-RAS Online Help - *Model Stability*. Retrieved February 2, 2008, from http://www.bossintl.com/online_help/hec-ras/source/modelstability3.htm.

Hoggan, D. H. (1989). *Computer-Assisted Floodplain Hydrology and Hydraulics*: McGraw-Hill, Inc.

IFRC. (2004). Philippines: Floods. Retrieved January 30, 2008, from http://www.ifrc.org/docs/appeals/rpts04/philippinesfloodsib0204.pdf.

Janssen, L. L. F. e., Huurneman, G. C. e., Bakker, W. H., Janssen, L. L. F., Reeves, C. V., Gorte, B. G. H., et al. (2001). *Principles of remote sensing : an introductory textbook* (Second edition ed.). Enschede: ITC.

JBIC. (2001). Pasig River Flood Warning System Project. Retrieved June 14, 2007, from http://www.jbic.go.jp/english/oec/post/2001/pdf/e_project_54_all.pdf.

Kassam, A., & Smith, M. (2001). FAO Methodologies on Crop Water Use and Crop Water Productivity. Retrieved January 29, 2008, from http://www.fao.org/landandwater/aglw/cropwater/docs/method.pdf.

Kobold, M., & Brilly, M. (2006). The use of HBV model for flash flood forecasting. *Natural Hazard and Earth System Sciences, 6*(3), 407-425.

Lindstrom, G., Johansson, B., Persson, M., Gardelin, M., & Bergstrom, S. (1997). Development and test of the distributed HBV-96 hydrological model. *Journal of Hydrology, 201*, 272-288.

Maidment, D. R. e. (1993). *Handbook of hydrology*. New York etc.: McGraw-Hill.

Miller, J. B. (1997). *Floods : people at risk, strategies for prevention*. New York etc.: United Nations, Department of Humanitarian Affairs.

NASA. (2005). SRTM Topography. Retrieved December 28, 2007, from ftp://e0srp01u.ecs.nasa.gov/srtm/version2/Documentation/SRTM_Topo.pdf.

NASA. (2006). NASA Facts: TRMM Instruments. Retrieved December 27, 2007, from http://trmm.gsfc.nasa.gov/overview_dir/pr.html.

Nash, J. E., & Sutcliffe, J. V. (1970). River flow forecasting through conceptual models : part I. a discussion of principles. *Journal of hydrology, 10*(3).

PAGASA. (2004). Climate of the Philippines. Retrieved November 2, 2007, from http://pagasa.dost.gov.ph/.

Perry, C. A. (2000). Significant Floods in the United States During the 20th Century - USGS Measures a Century of Floods [Electronic Version]. Retrieved March 2000 from http://ks.water.usgs.gov/Kansas/pubs/fact-sheets/fs.024-00.html.

Pike, J. (2000). Digital Terrain Elevation Data [DTED] [Electronic Version]. Retrieved December 28, 2007 from http://www.fas.org/irp/program/core/dted.htm.

ReliefWeb. (2007). Red Cross launches urgent appeal for flood hit Asia. Retrieved January 30, 2008, from http://reliefweb.int/rw/rwb.nsf/db900sid/KHII-75T2P7?OpenDocument.

Rientjes, T. H. M. (2007). Modelling in Hydrology (pp. 233): International Institute for Geo-information Science and Earcth Observation.

Rodriguez, E., Morris, C. S., Belz, J. E., Chapin, E. C., Martin, J. M., Daffer, W., et al. (2005). An assessment of the SRTM topographic products. Retrieved December 27, 2007, from http://www2.jpl.nasa.gov/srtm/srtmBibliography.html.

SMHI. (2006). Integrated Hydrological Modelling System Manual: SMHI.

Spitz, K., & Moreno, J. (1996). *A practical guide to groundwater and solute transport modelling*. New York etc.: Wiley & Sons.

Stowa/MX.Systems. (2004a). Duflow Modelling Studio: Duflow Manual, Version 3.7.

Stowa/MX.Systems. (2004b). *Duflow Modelling Studio: User's Guide, Version 3.7*.

Syed, K. H., Goodrich, D. C., Myers, D. E., & Sorooshian, S. (2003). Spatial characteristics of thunderstorm rainfall fields and their relation to runoff. *Journal of Hydrology, 271*(1-4), 1-21.

UNICEF. (2007). Retrieved Junuary 30, 2007 from http://www.unicef.org/emerg/india_40526.html.

USGS. (2006). Flood Hazards - A National Threat. from http://pubs.usgs.gov/fs/2006/3026/index.html

USGS. (2007). Science Topics. *Floods* Retrieved November 2, 2007, from http://www.usgs.gov/science/science.php?term=398.

WHO/Europe. (2002, September 13, 2002). FLOODING: Health effects and preventive measures. from http://www.euro.who.int/document/mediacentre/fs0502e.pdf.

WHO/Europe. (2007). Threats and challenges to health security in the WHO European Region. *Natural disasters and emergencies on the increase* from http://www.euro.who.int/Document/Mediacentre/fs0307e.pdf.

Wikipedia. (2007a). African Floods. Retrieved February1, 2008, from http://en.wikipedia.org/wiki/2007_African_floods.

Wikipedia. (2007b). Floods. Retrieved November 2, 2007, 2007, from http://en.wikipedia.org/

Zhang, W., & Montgomery, D. R. (1994). Digital elevation model grid size, landscape representation, and hydrologic simulations. *Water Resources Research, 30*(4), 1019-1028.

Appendix

Appendix A: List of Acronyms

DEM – Digital Elevation Model
DMS – Duflow Modelling System
DPWH – Department of Public Works and Highways
DTED – Digital Terrain Elevation Data
DUFLOW – Dutch Flow
EFCOS – Effective Flood Control and Operation System
EM-DAT – Emergency Disaster Data Base
ESCAP – Economic and Social Commission for Asia and the Pacific
FAO – Food and Agriculture Organization
GIS – Geographic Information System
HBV – Hydrologiska Byråns Vattenbalansavdelning (Hydrological Bureau Waterbalance)
IFRC – International Federation of Red Cross and Red Crescent Societies
KGPS – Kinematic Global Positioning System
MMDA – Metro Manila Development Authority
NAMRIA – National Mapping and Resource Information Authority
NASA – National Aeronautics and Space Administration
NGA – National Geospatial-Intelligence Agency
NHCS – Napindan Hydraulic Control System
PAGASA – Philippine Atmospheric, Geophysical and Astronomical Services Administration
SRTM – Shuttle Radar Topographic Mission
TRMM – Tropical Rainfall Measuring Mission
UN – United Nations
UNICEF – United Nations Children's Fund
WCI – Woodfields Consultants, Incorporated

Appendix B: Classification of Flood Phase

The Flood Phase is classified into four stages: Precautionary, Caution, Emergency and Post Flood. Each stage is defined as follows:

1. **Precaution Stage**
   This stage occurs when the water level at Sto Nino Water Level Gauging station is more than 13.0 m corresponding to 150 m^3/s.

2. **Caution Stage**
   This Caution Stage occurs in case the water level at Sto Nino Water Level Gauging Station is between critical water level 1 and 2.

3. **Emergency Stage**
   This stage occurs when the water level at Sto Nino Water level Gauging Station is more than critical water level 2.

4. **Post Flood Stage**
   The Post Flood Stage takes place when the water level at Sto Nino Water Level Gauging station is less than the critical water level 1.

   Critical Water level 1 is the allowable water level at Sto Nino Water Level Gauging Station before overbank flooding along Pasig-Marikina River, even if both the Rosario Weir and Napindan HCS are closed, so as not to increase the water level at Laguna Lake.

   Critical Water Level 2 is the allowable water level at Sto Nino Water Level Gauging Station before overbank flooding along Pasig-Marikina River, in case the Rosario Weir is fully opened and Napindan HCS is closed, to store the flood water into Laguna Lake for the bigger flood situation.

   The elevation of the critical levels 1 and 2 vary depending on the tidal level at the river mouth in Manila Bay.

Tidal Level	Critical Water Level (Sto. Nino)	
	1	2
Less than 10.6	15.6	17.1
10.6 to 10.8	15.5	17.0
10.8 to 11.0	15.5	16.9
11.0 to 11.2	15.4	16.7
11.2 to 11.4	15.3	16.6
More than 11.4	15.2	16.4

Source: CTI Engineering Co. LTD. (1993)

Appendix C: Principles of Flood Operation

The flood operation principle of each stage in flood phase, including that of non-flood phase is described in the following:

1. **Non-Flood Phase during Rainy Season**

   Rosario Weir and Napindan HCS are operated to decrease the water level of Laguna Lake as much as possible taking into account some other water utilization programs that the lake is subject to.

2. **Precautionary Stage in Flood Phase**

   Rosario Weir and Napindan HCS are operated to contain Laguna Lake water in the Pasig River.

3. **Caution Stage in Flood Phase**

   Napindan HCS is closed to store water into Laguna Lake. Rosario Weir is operated to divert flood water into Laguna Lake.

4. **Emergency Stage in Flood Phase**

   Rosario Weir and Napindan HCS are operated to decrease the water level of Pasig River, before flood in the city area occurs.

5. **Post Flood Stage**

   Rosario Weir and Napindan HCS are operated to decrease Laguna Lake water level as much as possible.

Source: CTI Engineering Co. LTD. (1993)

Appendix D: Flood Warning Announcements

ANNOUNCEMENT	CONTENTS
A	THIS IS A DISCHARGE WARNING FROM ROSARIO MASTER CONTROL STATION: ALTHOUGH GATE CLOSED, YOUR ATTENTION IS CALLED TO BE CAUTIOUS. FLOOD MAY OCCUR, SO KEEP OUT OF THE FLOODWAY CHANNEL.
B	THIS IS A DISCHARGE WARNING FROM ROSARIO MASTER CONTROL STATION: THE RELEASE OF WATER THROUGH THE ROSARIO FLOODGATES WILL NOW COMMENCE. THE SURGE OF WATER WILL BECOME SWIFT. THE PUBLIC IS ADVISED NOT TO GO NEAR THE FLOODWAY CHANNEL TO AVOID RISK.
C	THIS IS A DISCHARGE WARNING FROM ROSARIO MASTER CONTROL STATION: THE RELEASE OF WATER SHALL COMMENCE THROUGH THE ROSARIO FLOODGATES. THE LEVEL OF WATER WILL SOON RISE AND ITS FLOW WILL GRADUALLY BECOME SWIFT. THE PUBLIC IS ADVISED NOT TO GO NEAR THE FLOODWAY CHANNEL TO AVOID RISK.
D	THIS IS A DISCHARGE WARNING FROM ROSARIO MASTER CONTROL STATION: THE FLOODGATES OF ROSARIO HAVE NOW BEEN CLOSED. HOWEVER, THE PUBLIC IS REQUESTED TO REMAIN CAUTIOUS AND TO KEEP AWAY FROM THE FLOODWAY CHANNEL DUE TO THE POSSIBLE OCCURRENCE OF FLOOD.

Source: CTI Engineering Co. LTD. (1993)